Analysis of the effects of dike structures on heave failure at screens

Evaluation on the effects on hydraulic heave failure through an experimental heave screen setup and an analytical two-pressure stability model

Author: Lukas Raadschelders
External supervisor: Bas Berbee
Internal supervisor: Erik Horstman

29 June 2023

University of Twente | Fugro

UNIVERSITY OF TWENTE.

FUGRO

Preface

This Bachelor thesis report investigates the effects of dike structures on heave failure. These effects have been evaluated through an experimental heave screen setup and with an analytical two-pressure stability model. This research project was performed at the hydraulic engineering department of Fugro. During my bachelor thesis, I learned a lot about interesting subjects within hydraulic engineering in Civil Engineering. I got the chance to apply this knowledge in the performed experiments and the developed analytical model for the research project.

A special thanks to the supervisors from Fugro, Bas Berbee and Gert-Ruben van Goor. Their guidance and knowledge helped me to understand the theory and practicalities of the topic of hydraulic engineering within my thesis project. The company Fugro helped a lot in my thesis project with the possibility to make use of their lab facilities and provide the possibility for the development of an actual experimental setup. Also special thanks to my internal supervisors, Erik Horstman and Loreta Cornacchia. Loreta Cornacchia provided feedback in the first stages of the proposal of my thesis project. Erik Horstman provided further guidance and detailed feedback throughout the thesis project.

Lastly, I hope you will enjoy reading my thesis report about the analysis of the effects of dike structures on heave failure at screens. If any questions about the project arise, please feel free to contact me.

Lukas Raadschelders

l.t.raadschelders@student.utwente.nl

Contents

Figures in the Main Text

Tables in the Main Text

Abstract

In the upcoming years, the network of dikes and levees in the Netherlands will be reinforced to meet the new safety norms for dikes. One crucial failure mechanism for dikes is the piping failure mechanism. The placement of a heave screen is a reinforcement method to reduce the risk of piping at a dike. This reinforcement method introduces another possible failure mechanism: hydraulic heave failure. This research project investigates the effects of dike structures on hydraulic heave failure. Two phenomena related to dike structures can be distinguished which influence hydraulic heave failure: the effects of vertical loading of a dike structure on heave failure and the effect of the occurrence of piping on heave failure. Both these effects have been analysed with a two-dimensional analytical two-pressure model and through an experimental design of a heave screen.

The analytical two-pressure model is a computation model which determines the two main pressures in the process of heave failure. Namely, the total downward soil pressure and the total upward seepage pressure. In this two-pressure analytical model, the effects of vertical loading and the occurrence of piping have been integrated. The analytical model is then used to compute the different experimental scenarios. The experimental design is constructed as a representation of a scaled version of a dike structure with a heave screen. In this experimental setup, multiple experimental scenarios are recreated to investigate both effects of a dike structure and piping on heave failure.

The analytical two-pressure model and the experimental model of a heave screen are compared with quantitative and measurable variables. The critical upstream water height is the critical point for hydraulic heave failure to occur both analytically and experimentally. Analytically, this critical point of failure can also be expressed as the factor of safety. Experimental and analytical results on the critical upstream water height are plotted compared to the applied vertical loading by the dike structure. From these results, conclusions can be drawn on the relationship between the critical point of hydraulic heave failure and the applied vertical load.

The analytical results show a clear positive correlation between the critical upstream water height and the applied vertical load. The experimental results, however, show a weak positive correlation was found between both variables. Therefore, it is concluded that the resistance against heave failure is positively correlated with the vertical loading of a dike structure. However, it should be noted that for the quantification of the effect of vertical top load on heave failure further experimental research is recommended.

This study introduces the meso scale analysis on heave failure. The effects of the occurrence of piping on heave failure are investigated on meso scale. The meso scale analysis shows specific locations in the heave zone for which heave failure could already occur before the macro scale analysis indicates heave failure. The comparison of experimental and analytical results shows a relation between the pipe width and the critical point of heave failure. This suggests a direct relation between piping and heave failure at heave screens. Therefore, further research into this relation is recommended before a concrete conclusion substantiated by a calculation model can be formulated on the effects of the occurrence of piping on heave failure.

1. Introduction

The Netherlands has a large network of dikes and levees. Structural safety of these structures is crucial for future safety of all lower lying areas in the Netherlands. Piping is a failure mechanism that can bring the structural safety of dikes into danger. Especially, dikes constructed on a sand layer are vulnerable to hydraulic failure caused by piping. Therefore, heave screens can be implemented at dikes as a reinforcement measure against piping. Heave screens increase the piping length and thus decrease the chance of hydraulic failure caused by piping. The implementation of heave screens at dikes introduces a new failure mechanism for stability of dikes, hydraulic failure caused by heave. Heave failure can be described as the liquification of the soil caused by the upward seepage flow around the downstream side of the heave screen. This liquification of the soil results pipe growth below the heave screen. Eventually, the pipe growth will lead to failure of the dike structure on top.

Currently, the design criteria for a heave screen against heave failure are based on a situation with a sheet pile and an open water level on both sides of the sheet pile. This situation has crucial differences compared to a dike structure with an implemented heave screen. Consequently, the current design criteria may not be appropriate for the design of a heave screen under a dike. In Figure 1.1 and Figure 1.2, both situations are visualised. This thesis research explores the effects of dike structures on heave failure. In this study, two scientific approaches for analysing the effects of dike structures on heave failure are featured. The first approach presents an analytical solution on heave failure. This analytical solution is based on existing theories on heave at a screen. This solution is then extended with a calculation method for considering the effects of dike structures on top of the heave screen. The analytical solution is compared with experimental results. These results follow from experiments in a scaled experimental setup. The analytical and experimental results are used to draw conclusions on the research questions and on the general research objective.

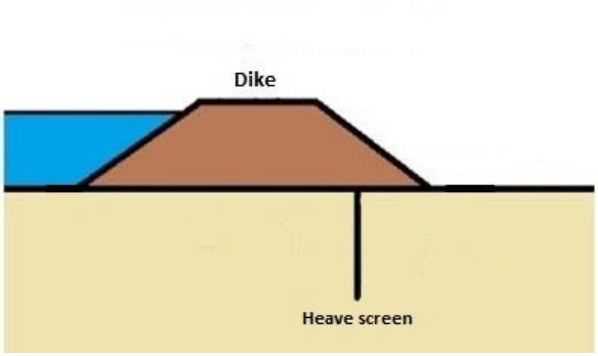

Figure 1.1: Schematic dike structure with heave screen (Oldhoff, 2013, modified)

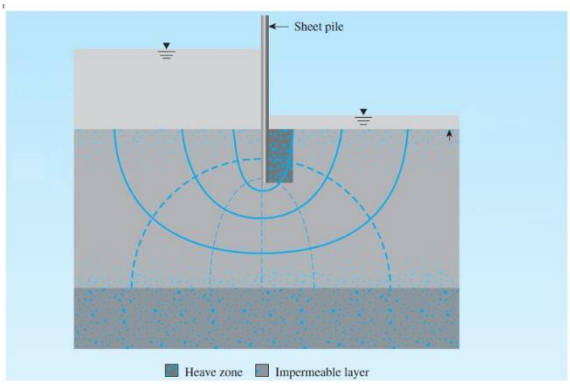

Figure 1.2: Seepage flow net around a sheet pile with two open water levels (Das & Sobhan, 2013, modified)

2. Research context & framework

2.1 Current application and design of heave screens

Heave screens are a type of sheet piles that are applied at dike structures. Heave screens are typically designed to strengthen the dike against the failure mechanism piping. These heave screens lengthen the piping distance, which is the distance a growing pipe needs to travel to reach the other side of the dike. Therefore, the piping failure mechanism is less likely to occur with an increasing piping distance due to the introduction of the heave screen. This makes the dike less vulnerable to failure because of piping. This is schematically visualised in Figure 2.1 and Figure 2.2. In Figure 2.1, a pipe is shown which formed along the heave screen. In Figure 2.2, a pipe is shown below a dike without a heave screen.

The piping failure mechanism is generally well-described with the mathematical model of Sellmeijer for piping (Förster et al., 2012). However, in Figure 2.1 can be seen that with the application of a heave screen at a dike, the groundwater seepage flow ("occurrence of piping") does not only travel in horizontal direction. Near the heave screen, the pipe travels vertically. Therefore, the heave phenomenon can occur. Heave can be described as the liquification of the soil caused by the upward seepage flow around the lower side of the heave screen. The mathematical model of Sellmeijer only describes the piping in horizontal direction. The model of Sellmeijer is therefore insufficient for a full analysis on the failure mechanisms caused by groundwater flow (Förster et al., 2012).

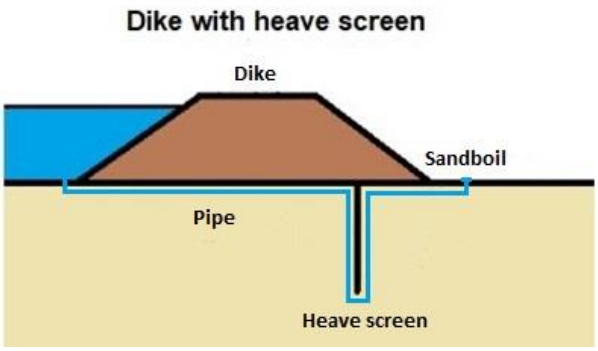

Figure 2.1: Piping mechanism at a dike with a heave screen (Oldhoff, 2013, modified)

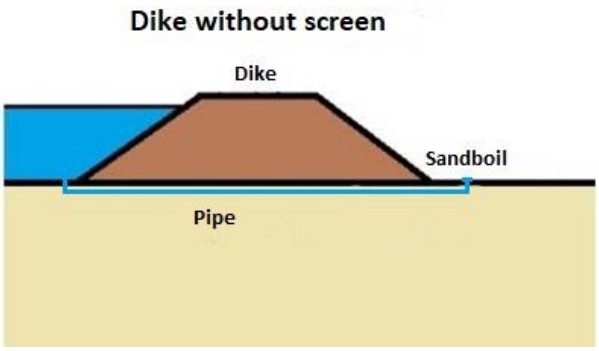

Figure 2.2: Piping mechanism at a dike without a heave screen ((Oldhoff, 2013, modified)

Currently, the heave process is modelled with a mathematical model that is based on the situation where there is a sheet pile with a water level on both sides (depicted in Figure 1.2) (Terzaghi, 1922; Garai, 2016). This mathematical framework of the heave process is discussed in detail in Chapter 3.2. For the design of heave screen against heave failure in the Netherlands, a standard design criterium is set. This design criterium is called the heave criterium. This heave criterium is based on the critical hydraulic gradient in the mathematical model of the heave process (Förster et al., 2012). The hydraulic gradient can be explained as the driving force for groundwater seepage through soil. The critical hydraulic gradient characterizes the maximum value for seepage stability in a soil fragment (Quanyi et al., 2018).

2.2 Relevance of a study into heave failure at heave screens

For the geotechnical consultant Fugro, this research into heave failure creates an interesting opportunity. In the upcoming years, dike structures in the Netherlands need to be reinforced for different failure mechanisms. Currently, 1565 kilometres of the primary dike structures in the Netherlands need to be reinforced to comply with the national norms for flood safety (Hoogwaterbeschermingsprogramma, 2017). The failure mechanism piping is an important failure mechanism for dikes in the Netherlands (Wiggers et al., 2022). Piping can ultimately lead to the failure of dikes because of erosion of the soil layer below the dike structures (Förster et al., 2012). The application of heave screens against piping can be a possible solution for the reinforcement of dikes against failure due to piping. However, the current design approach for heave failure at heave screens for dikes falls short considering the effects of the dike structure and the occurrence of the failure mechanism of piping.

This research examines the impact of dike weight and the impact of piping on heave failure and aims to determine whether this impact can be categorized as positive or negative in terms of heave screen design. It is possible that the current design process for heave screens creates over-sized heave screens. This would be the case if the top load of a dike reduces the chance of heave failure to occur at a heave screen. Conversely, if the presence of a dike speeds-up the occurrence of heave failure, the current design process of heave screens would be insufficient. In this case, for instance, heave failure would occur faster at a pipe than with an open water potential at both sides of the heave screen because of the differences in groundwater flow. To conclude, there are plentiful possible effects that can influence the heave failure mechanism at dike structures. This highlights the importance of the research into the effects of dike structures on heave failure for the future application of heave screens in dikes.

2.3 Research problem description

Deltares defined calculation model for the prevention of heave failure at screens below dike structures: the heave criterium (Förster et al., 2012). This heave criterium is based on the stability criterion defined by Terzaghi (Terzaghi, 1922). This stability criterion is intended to design solutions for the prevention of heave failure at sheet piles in a situation with non-cohesive soils below (variable) open water levels at both sides of the sheet pile (shown in Figure 1.2). The stability criterion does not represent a dike structure with a heave screen (schematically depicted in Figure 1.1). If these two situations are compared to each other in the scope of the heave failure mechanism, two important differences can be observed:

- The top load of the dike structure on the soil instead of a free water surface near the sheet pile
- The presence of a pipe as a local open water potential instead of a general open water level

The effect of these two differences on the occurrence of the heave failure mechanism are yet to be determined. The current design stability criterion does not consider these two effects. Consequently, the stability criterion of Terzaghi may not be appropriate for the design of heave screens at dike structures. This thesis project studies the effects of dike structures on heave failure to provide a scientific analysis of these effects in the scope of heave failure as defined by the stability criterion.

2.4 Research objective

The objective of this thesis project is to assess the effects of the occurrence of piping and the loading of a dike structure on heave failure at heave screens.

Along with the research objective, a hypothesis can be formulated for the analysis of the effects of piping and the loading by a dike structure on heave failure at heave screens. It is hypothesized that the top load of a dike structure increases the vertical pressure exerted by the submerged weight of the soil at the heave screen. The occurrence of piping as local open water potential creates a more concentrated outflow of groundwater. This lowers the resistance for heave failure to occur than a general open water level. Therefore, the top load of the dike increases the resistance for heave failure and the occurrence of piping decreases the resistance for heave failure. Both effects combined there is hypothesized that effects of dike structures potentially decrease the chance for heave failure to occur compared to a situation without piping and an increased surface load.

2.5 Research questions

How can existing analytical equations on heave failure be used to consider the effects of dike structures with heave screens on heave failure?

a. How does the top load of the dike structure affect the heave failure mechanism?
b. How does the presence of a pipe below a dike structure, acting as a local open water potential, affect the heave failure mechanism?
c. What equilibrium condition for the soil needs to be applied for heave at heave screens in/under dike structures?

How do trends in experimental results of heave failure at dike structures with heave screens compare to predictions following from existing analytical solutions?

a. What critical thresholds for the occurrence of heave are observed in experiments for heave failure at dike structures?
b. How do the results of the experiments for heave failure at dike structures with heave screens compare to the results of the analytical equations

3. Theoretical framework

3.1 The fundamentals of heave in soil

Hydraulic heave is a phenomenon that can be characterised as a vertical seepage flow through soil, ultimately lifting soil out of the surface layer. Heave is caused by a pressure potential due to a water level difference. For heave to occur it is essential that the soil layer is permeable. In Figure 3.1, heave is schematized around a sheet pile. Here the potential in water level is the difference in the water level at both sides of the sheet pile. Seepage flow therefore occurs from the high-water level to the lower water level. In the figure, this vertical seepage flow is displayed by a line with arrows that indicate the flow direction.

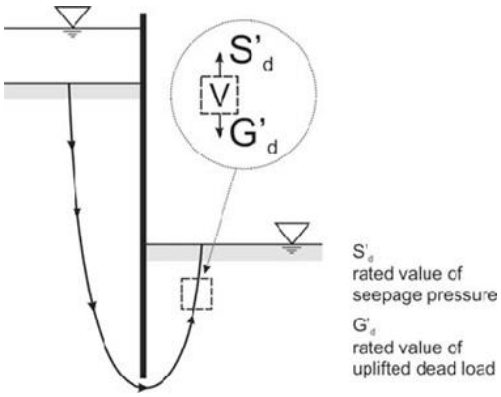

Figure 3.1: Schematic visualisation of pressures in soil caused by heave (Wudtke, 2008)

Different pressures act on a soil fragment (*V*) located in the seepage flow. Globally, these pressures can be divided into two main pressures, namely the upward seepage pressure of the soil fragment (S'_d) and the downward soil pressure of the soil fragment (G'_d)[1]. These two pressures are also shown two-dimensional in Figure 3.1. The soil fragment is kept together by the net effect of both pressures. If the upward seepage pressure increases, the grain tension in the soil fragment decreases. This causes the liquification of the soil in the fragment. Ultimately, the soil will be completely liquified and a "quicksand" and "sand boiling" situation occurs (Förster et al., 2012). This complete process is called "heave" or "hydraulic failure caused by heave". Heave can cause the loss of stability of the surrounding soil and potential structures.

3.2 Hydraulic failure caused by heave

Hydraulic failure caused by heave can be examined with equilibrium equations. These equilibrium equations can be divided in global equilibria where the stability of a soil aggregate is examined and a local equilibrium where the stability of a soil grain is examined. A soil aggregate is defined here as a rectangular volume of soil particles. A soil grain is defined as one soil particle.

[1] In literature, the definition of the variables S'_d and G'_d as pressure or force differs. In this study, variables S'_d and G'_d are defined as pressures. In the study, all calculated pressures work over the same area. Therefore, there is no relative difference in computing pressures or forces for S'_d and G'_d

3.2.1 Global heave stability criterion

Liquification caused by heave can be seen as hydraulic failure of the soil. If the soil completely liquifies, the soil layer loses all structural stability. As explained in Chapter 3.1, pressures acting on the soil aggregate can be divided into two main pressures. These two pressures constitute a global equilibrium acting on the soil aggregate. According to Garai, three global equilibria can be determined for a soil aggregate subjected to heave. These three equilibria equations form the stability criterion for a soil aggregate (Terzaghi, 1922) (Garai, 2016).

1. $S'_d < G'_d$ 3.1

2. $\mathrm{u} < \sigma_z$ 3.2

3. $\mathrm{i_z} < \mathrm{i_c}$ 3.3

Where,
S'_d is the upward seepage pressure [kN/m^2]
G'_d is the downward soil pressure [kN/m^2]
i_z is the hydraulic gradient in vertical direction [-]
i_c is the critical hydraulic gradient [-]
u is the destabilizing pore water pressure [kN/m^2]
σ_z is the stabilizing vertical pressure [kN/m^2]

The stability equation 3.1 corresponds with the two acting pressures displayed in Figure 3.1. If the upward seepage pressure remains smaller than downward soil pressure of the soil aggregate, the soil aggregate cannot be lifted out of the surface layer. The stability equation 3.2 concerns the internal grain tension within the soil aggregate. If the pore water pressure stays smaller than the total vertical stress, the soil aggregate maintains its internal stability and the "quicksand" situation cannot occur. The stability equation 3.3 describes the stability of soil aggregate in terms of the hydraulic gradient. The hydraulic gradient is defined as the driving force for hwater seepage through soil. The critical hydraulic gradient characterizes the maximum value for seepage stability in a soil aggregate (Quanyi et al., 2018). If the vertical hydraulic gradient stays smaller than the critical hydraulic gradient, the seepage stability of the soil aggregate will remain sufficient.

The critical hydraulic gradient stated in the stability equilibrium 3.3 can be determined with two definitions according to literature. The first definition uses the unit weight of the soil particles and the value for the porosity to determine the critical hydraulic gradient (Förster et al., 2012; Garai, 2016). The second definition uses the unit weight of the saturated soil for the critical hydraulic gradient (Das & Sobhan, 2013).

$$Definition\ 1: \quad i_c = \frac{(1-n)(\gamma_s-\gamma_w)}{\gamma_w} \qquad 3.4$$

$$Definition\ 2: \quad i_c = \frac{\gamma_{sat}-\gamma_w}{\gamma_w} \qquad 3.5$$

Where,
n is porosity value of the soil [-]
γ_s is unit weight of the soil particles [kN/m^3]
γ_{sat} is the unit weight of the saturated soil [kN/m^3]
γ_w is the unit weight of water [= 9,81 kN/m^3]

Both the definitions give similar results for the hydraulic gradient and are stated here below. In this study, the second definition of the critical hydraulic gradient is used in further analyses.

The three stability equilibria can be further elaborated with corresponding equations for the terms in the equilibria. Therefore, the stability criterion can be rewritten (Das & Sobhan, 2013) (Förster et al., 2012).

1. $S'_d = \sigma_{seep} + u < G'_d = \sigma_{z,total}$ 3.6

2. $u = \gamma_w * \mathrm{D}_{\mathrm{screen}} < \sigma_z = \gamma_{sat} * \mathrm{D}_{\mathrm{screen}}$ 3.7

3. $i_z = \frac{\Delta\varphi}{D_{screen}} < i_c = \frac{\gamma_{sat}-\gamma_w}{\gamma_w}$ 3.8

Where,
D_{screen} is the depth of the heave screen measured from the top of the soil [m]
$\Delta\varphi$ is the difference in hydraulic head between the top of the soil and the bottom at heave screen [m]
σ_{seep} is the seepage pressure at the bottom of the heave screen [kN/m^2]
$\sigma_{z,total}$ is the total downward vertical pressure at the bottom of the heave screen [kN/m^2]

3.2.2 Local heave stability criterion

Zooming in on a single soil grain within the soil aggregate, a stability equilibrium can be determined with the forces acting on this specific soil grain. These forces are caused by the upward flow of water (v_w) determined by Darcy's law for seepage velocity (Darcy, 1856) and the effective velocity of a "falling" soil grain (v_t) estimated with Stokes law (Cistin, 1966). In Figure 3.2, the stability of soil grains is shown.

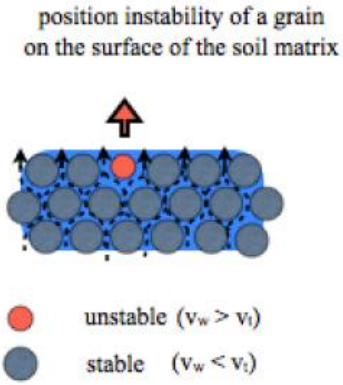

Figure 3.2: Stability forces on soil grains in a soil matrix of a non-cohesive soil (Garai, 2016)

Darcy's law for seepage velocity and Stokes law for the effective velocity of a "falling" sphere can be combined into an equilibrium condition for a soil grain. This stability condition is stated in the equation below (Kovks, 1981; Garai, 2016).

$$i_z < cd^2 \quad \text{with} \quad c = \frac{n(\rho_s - \rho_w)g}{36 k_z \mu} \tag{3.9}$$

Where,
c is the defined constant of soil parameters
ρ_s is the density of the soil particle [= 2650 kg/m^3 (Verruijt, 2001)]
ρ_w is the density of the water [= 1000 kg/m^3]
g is the gravitational acceleration [= 9,81 m^2/s]
d is the soil particle diameter [m]
μ is the viscosity of water [= 0.0015 kg/ms]
k_z is the hydraulic conductivity of the soil in vertical direction [m/s]
i_z is the hydraulic gradient in vertical direction [-]
n is the porosity of the soil [-]

In Equation 3.9, can be seen that for a soil with constant properties, constant *c* can be determined and the soil particle diameter and the hydraulic gradient are the only variables. Equation 3.9 can be rewritten to determine the soil particle diameter for a given hydraulic gradient.

$$d = \sqrt{\frac{i_z}{c}} \text{ with } c = \frac{n(\rho_s - \rho_w)g}{36 k_z \mu} \tag{3.10}$$

This soil particle diameter is important for the local stability condition. Therefore, the soil particle diameter can be calculated for a critical hydraulic gradient. For a critical hydraulic gradient, this will be the critical soil diameter. This is shown in Equation 3.10 (Garai, 2016; Das & Sobhan, 2013).

$$d_c = \sqrt{\frac{i_c}{c}} = \sqrt{\frac{\gamma_{sat} - \gamma_w}{c\gamma_w}} \tag{3.11}$$

Where,
d_c is the critical diameter of the soil particle [m]
i_c is the critical hydraulic gradient [-]

If the soil diameter is smaller than the critical soil diameter for the critical hydraulic gradient. The soil particle will lose its stability in the soil matrix (which can be seen in Figure 3.2. indicated by the red arrow). The loss of the stability of a soil particle has a cascading effect on the stability of other soil particles in a soil aggregate. Eventually this will result in an irreversible situation where multiple soil particles come loose and the stability of the whole soil aggregate will be lost (Garai, 2016). Therefore, it can be concluded that the global equilibria are not sufficient to assess for the occurrence of heave. Especially, Equation 3.1 for global stability which assesses the hydraulic gradient, is insufficient if the critical soil diameter is exceeded. The article of Garai, therefore, describes the following extra step for

the assessment of heave. If the soil particle diameter is smaller than the critical soil diameter, heave can occur because of failure of the local soil particle equilibrium. If the soil particle diameter is larger than the critical soil diameter, the soil fragment can be assessed on the heave failure mechanism with the three global stability equilibria (Garai, 2016).

3.3 Factor of safety for heave failure mechanism at sheet piles

In the previous sections, heave failure is discussed with local and global stability conditions. The global stability condition can be assessed for a certain soil aggregate in the study area around the sheet pile. Terzaghi found that hydraulic failure caused by heave generally occurs in a specific zone near the sheet pile (Terzaghi, 1922). This specific zone is called the heave failure zone and is depicted in Figure 3.3. This heave failure zone is defined by the soil depth of the sheet pile (*D*) and half of the sheet pile depth (*D/2*) for its width (Terzaghi, 1922).

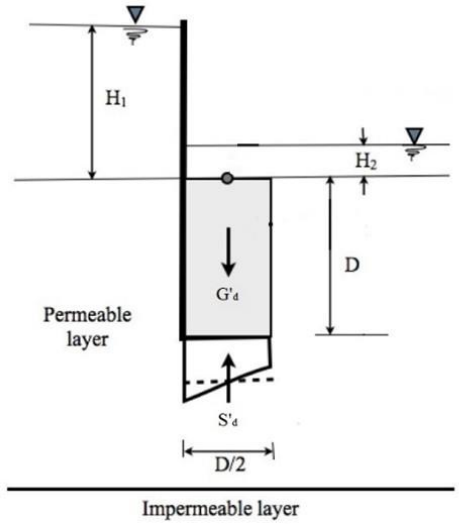

Figure 3.3: The heave failure zone (Garai, 2016, modified)

For the design of sheet piles against heave failure, a factor of safety can be used. This factor of safety for heave derived from Figure 3.3 is described with Equation 3.12 (Das & Sobhan, 2013). This factor of safety is a ratio between the total downward soil pressure and the total upward seepage pressure. For an increased factor of safety, the chance that heave failure will occur on the heave failure zone is lower. The soil and seepage pressure are derived from stability equation 3.1.

$$FS = \frac{G_d'}{S_d'} = \frac{\sigma_{z,total}}{\sigma_{seep} + u}$$

3.12

Definition for total downward soil pressure: $\sigma_{\mathrm{z,total}} = \gamma_{\mathrm{sat}} * D_{screen} + \gamma_{\mathrm{w}} * H_2$

3.13

Definition for the total upward seepage pressure: $\sigma_{\mathrm{seep}} + \mathrm{u} = \gamma_{\mathrm{w}} * \mathrm{i_z} * \mathrm{D} + \gamma_{\mathrm{w}} * (\mathrm{H_2} + \mathrm{D_{screen}})$

3.14

Where,
H_2 is the height of the water level downstream [m]

3.4 Vertical stresses in a soil layer

The heave failure mechanism is currently determined according to the situation shown in Figure 3.3. For an analysis of the effect of the top loading of a dike on the occurrence of heave, this section will discuss the vertical stress distribution model. Multiple solutions exist for stress distributions dependent on the type of vertical loading on the soil layer. All solutions for different types of loading are derived from the Boussinesq theory on vertical stress distribution in soil (Boussinesq, 1883). In this study, the solution for vertical stresses in a uniformly loaded rectangular area is discussed. Only this solution is elaborated since this study applies rectangular loads in the experiments (further explained in Chapter 5.4).

The theory of Boussinesq about vertical stress in soil caused by a rectangular load is derived from the solution for vertical stresses exerted by a point load. This solution describes an increase in vertical stress depending on the depth and radial distance from the point load (Das & Sobhan, 2014). Boussinesq's solution for a stress caused by a point load on soil included solutions for the x-component, y-component and the z-component. The z-component is the vertical stress component, the only component that will be considered. The vertical stress in soil caused by a point load is shown in Equation 3.15.

$$\Delta\sigma_z = \frac{3P}{2\pi}\frac{z^3}{L^5} \tag{3.15}$$

Where,
$\Delta\sigma_z$ is the vertical stress increase at a specific point in the soil [kN/m^2]
P is the point load [kN]
z is the depth for which the vertical stress is calculated [m]
L is $\sqrt{x^2 + y^2 + z^2}$ where, x and y are distance coordinates for a determined location [m]

Equation 3.15 can be rewritten to an equation for rectangular loads. Therefore, P needs to be substituted with $q\ dx\ dy$. Substituting and integrating Equation 3.15 yields the following equation (Das & Sobhan, 2013). This equation is derived to determine the value for vertical stress below the centre of the rectangular load.

$$\Delta\sigma_z = \frac{2\sigma_z}{\pi}\left(\frac{m*n}{\sqrt{1+m^2+n^2}} * \frac{1+m^2+2n^2}{(1+n^2)(m^2+n^2)} + \sin^{-1}\frac{m}{\sqrt{m^2+n^2}*\sqrt{1+n^2}}\right) \tag{3.16}$$

Where,
σ_z is the vertical load [kN/m^2]
$m = \frac{L}{B}$ with $L \geq B$
$n = \frac{z}{1/2 * B}$
L is the length of a rectangular load [m]
B is the width of a rectangular load [m]
z is the depth of the determined location for the solution on vertical stress [m]

Essential here is that the vertical stress theory of Boussinesq only applies for soil as medium. In case of seepage flow pipes in a soil layer, the vertical stress distribution through the soil layer will be disrupted. This means that the soil located directly under a formed pipe is less subjected to vertical stress for vertical loading on top of the soil.

4. Analytical model on hydraulic heave failure

4.1 Development of the analytical model

The analytical methodology consists of a method to find an analytical solution for the stated research objective. This analytical solution is computed with a two-pressure model. The model is mathematically built up from the theory on stability criteria for heave and vertical stresses presented in Chapter 3. The objective of this analytical solution is to combine the theory on hydraulic failure caused by heave, described with global stability conditions with the theory on vertical stresses in a soil layer. In this chapter, the development of the analytical model is discussed. In Appendix A, the model code of the analytical model is MATLAB is shown.

This analytical approach links to the first research sub-question with the aim to determine an analytical solution on heave failure considering the effects of the weight of dike structures. This analytical solution further includes an assessment of the effects of piping on hydraulic heave failure. This links to the second sub-research question stated in this study. As the piping phenomenon primarily affects smaller scale soil sample then hydraulic heave failure, the model incorporates varying levels of detail. These levels of detail also clearly distinguish assessment on local heave failure and global heave failure. The levels of detail are the micro scale, meso scale and macro scale. The micro scale is used to assess heave failure on soil particle level, whereas the macro scale is used to assess heave failure for the heave zone. The intermediate meso scale is used to analyse the stability of smaller soil aggregates in the heave failure zone (fragmented soil aggregates). This meso scale is suitable for assessing the effects of a single pipe on heave failure as it assesses smaller soil aggregates within the heave failure zone. The different levels of detail are schematically displayed in Figure 4.1.

The developed analytical two-pressure model is used to determine critical failure points for different loading conditions for which hydraulic heave failure occurs. These loading conditions in the analytical model are the same as the experimental scenarios that will be considered in Chapter 5. The critical failure points for these scenarios are determined with the local and combined global stability criteria. From these stability criteria, critical soil parameters for heave can be derived. These critical soil parameters can be quantified in the analytical model and correspond to critical conditions for the occurrence of heave failure.

The critical conditions for the occurrence of heave failure are quantified by critical upstream water levels. The critical upstream water level is defined as the water level for which heave failure occurs on the downstream side of the heave screen (for example, the critical upstream water level in Figure 3.3 is parameter H_1). The results on critical upstream water levels are evaluated at every level of detail. This gives insight in a decisive equilibrium condition for hydraulic heave failure as stated by the third research sub-question. The critical upstream water level is a measurable variable in the experimental setup. Therefore, this critical upstream water level can be compared to the critical upstream water level acquired from the experiments. The experimental setup is discussed in Chapter 5.

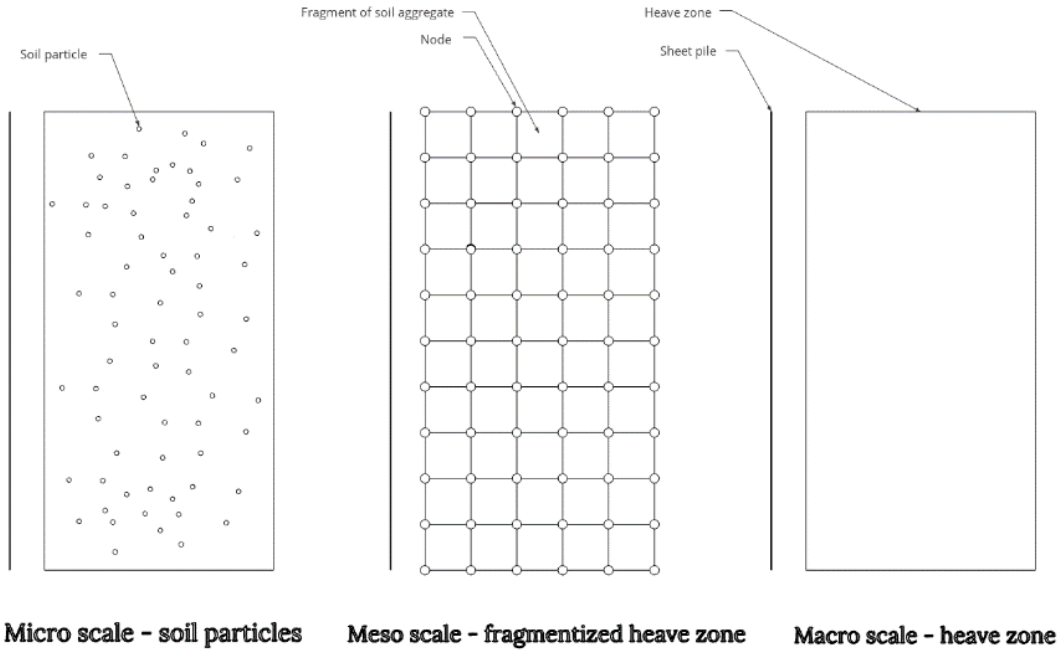

Figure 4.1: Levels of detail in analytical two-pressure model (left line represents heave screen, rectangular area represents heave failure zone)

4.2 Modelling the stability criteria

4.2.1 Local stability criterion – micro scale

The local stability criterion describes the stability of a soil particle in a soil layer. Therefore, the analytical model determines the critical soil particle diameter (d_c) for which a soil particle is unstable for the critical hydraulic gradient. If the soil contains particles with a smaller diameter, hydraulic heave failure can occur before the critical hydraulic gradient is exceeded. For the calculation of the critical soil particle diameter, Equation 3.11 is implemented in the model. The critical soil particle diameter (d_c) is then compared to the minimum soil particle diameter in the soil particle size distribution ($d_{min\ particle}$). If the minimum soil particle diameter is smaller than the critical soil particle diameter, local hydraulic heave failure occurs. Soil parameters in Equation 3.11 and the minimum soil particle diameter are determined with a laboratory test for the soil samples used in the experiments. These laboratory results are discussed in detail in Section 5.5

4.2.2 Global stability criterion – meso scale & macro scale

The global stability criterion defines the stability of a soil aggregate in the soil layer. The stability is defined with the three stability equations stated in Section 3.2.1. From these stability equations, critical soil parameters and heave equation parameters for the occurrence of heave failure can be computed. In Table 4.1, the local and global heave equation parameters and critical soil parameters and their point of failure are summarized for a clear overview. In the section below these parameters are explained.

Table 4.1: Heave equation & critical soil parameters

Level of detail	Heave equation parameters	Critical soil parameters	Point of failure
Local stability criterion	Minimum soil particle diameter ($d_{min,\ particle}$)	Critical soil particle diameter (d_c) (Eq. 3.11)	$d_{min,particle} \leq d_c$
Global stability criterion	Vertical hydraulic gradient (i_z) (Eq. 3.8)	Critical hydraulic gradient (i_c) (Eq. 3.8)	$i_z \geq i_c$
Global stability criterion	Total downward soil pressure (G'_d) (Eq. 3.13 and 4.4) Total upward seepage pressure (S'_d) (Eq. 3.14)	Factor of safety (*FS*) (Eq. 3.12)	$FS < 1$
		Excess seepage pressure (S'_{excess})	$S'_{excess} > 0$

Stability equation 3.1

The critical soil parameter is derived as the ratio of the total downward soil pressure (G'_d) and the total upward seepage pressure (S'_d). If the seepage pressure exceeds the soil pressure, the stability equation no longer holds. This critical point can be expressed in a ratio of the total soil pressure and the total seepage pressure. This ratio is the factor of safety (*FS)*. This factor of safety and both pressures are determined with Equation 3.12. If the factor of safety is below one, the seepage pressure is larger than the soil pressure and therefore heave failure may occur. Another way to express the relationship between both the pressures is by subtraction. In this subtraction, the total downward soil pressure is subtracted from the total upward seepage pressure. For this subtraction applies that a value below zero means that the total downward gsoil pressure pressure is larger. Therefore, the soil aggregate is stable. A value above zero indicates the excess seepage pressure (S'_{excess}) for which heave failure can occur. Important to state is that if an extra vertical load is added on the surface of the soil, this must be considered when computing the total downward soil pressure. The vertical stress increase component is calculated with Equation 3.16. This component is then added to the total downward soil pressure (G'_d). This calculation is further explained in the Section 4.4.

In theory, the global stability criterion is applicable for variable sizes of a soil aggregate. Therefore, the global stability criterion can also be applied for smaller fractions within the heave zone. This evaluation of the soil and seepage pressure on a smaller scale provides a more comprehensive understanding of the pressure distribution within the heave zone. This is because the total soil and seepage pressure increases over the depth. Also, the hydraulic gradient varies across the heave zone due to a varying hydraulic head along the heave screen. Therefore, at that meso scale the soil parameters are determined for multiple points in a grid in the heave zone. These points in the grid are the nodes. Every node is equally spaced from each other by a defined grid size (D_{grid}). In the middle illustration in Figure 4.1, an example of a grid with nodes in the heave zone is shown. An example of the display of the results of a heave equation parameter on the meso scale is shown in Figure 4.3. In this example, every node displays a value for the total seepage pressure. The values of surfaces in between are estimated with the interpolation function of MATLAB.

At the macro scale, the global heave equation parameters are determined over this complete heave zone. This implies that the vertical hydraulic gradient is determined at the lowest point of the heave zone, thus the depth of the heave screen. The same applies for the total downward soil pressure with optional extra vertical stresses and the total seepage pressure. For convenience, all heave equation parameters are determined at the center of the width of the heave zone ($1/4 * D$). This calculation point is approximately equal to the average of the full width of the heave zone (see Figure 3.3).

Stability equation 3.2

In this study, stability equation 3.1 broadly corresponds to stability equation 3.2. This can be seen when Equation 3.7 is compared with Equation 3.6 and its derivations of the stresses stated in Equation 3.13 and 3.14. The Equation 3.13 and 3.14 covers all soil parameters used in the stability equation 3.1 and 3.2. Therefore, the conclusion can be drawn that the stability equation 3.2 is satisfied if stability equation 3.1 is satisfied.

Stability equation 3.3

In this stability equation the critical soil parameter is the critical hydraulic gradient. In the analytical model, the critical hydraulic gradient is calculated with Equation 3.5. The critical hydraulic gradient is compared to the vertical hydraulic gradient in the model. The vertical hydraulic gradient (i_z) is determined with Equation 3.8. For this equation, the difference in hydraulic head ($\Delta\varphi$) needs to be determined. The values for hydraulic head along a heave screen are determined with the Deltares software MSeep. The explanation of the computations performed in Deltares MSeep is further discussed in Section 4.3.

4.3 Modelling the hydraulic head (Deltares MSeep)

The vertical hydraulic gradient (i_z) is used in the global stability criterion for the comparison to the critical hydraulic gradient and for the calculation of the total seepage pressure (S'_d). The hydraulic gradient is calculated with Equation 4.1 (the general form of Equation 3.8).

$$i_z = \frac{\varphi_p - \varphi_0}{x_p} \qquad 4.1$$

Where,
φ_0 is the hydraulic head at reference point [m]
φ_p is the hydraulic head at point P in vertical direction [m]
x_p is the distance between the reference point and point p [m]

The value for the hydraulic head at specific points in the heave failure zone are determined with the numerical model Deltares MSeep. This numerical model generates a 2D flow net around the heave screen with equipotential lines. This 2D flow net is generated based on the dimensions of the experimental model. An example of a flow net from MSeep generated based on the experimental model is given in Figure 4.2. It is Important to state that Deltares MSeep is developed for generation of flow nets in dimensions of meters. However, if the dimensions of the experimental model are expressed in meters. The dimensions of the flow net become too small for calculation in the numerical model. Therefore, the dimensions of the experimental model in centimeters are directly inserted in the model as meters. The output values for the hydraulic head are later scaled back to the correct units. This intermediate step does not influence the calculation of the hydraulic head in the numerical model.

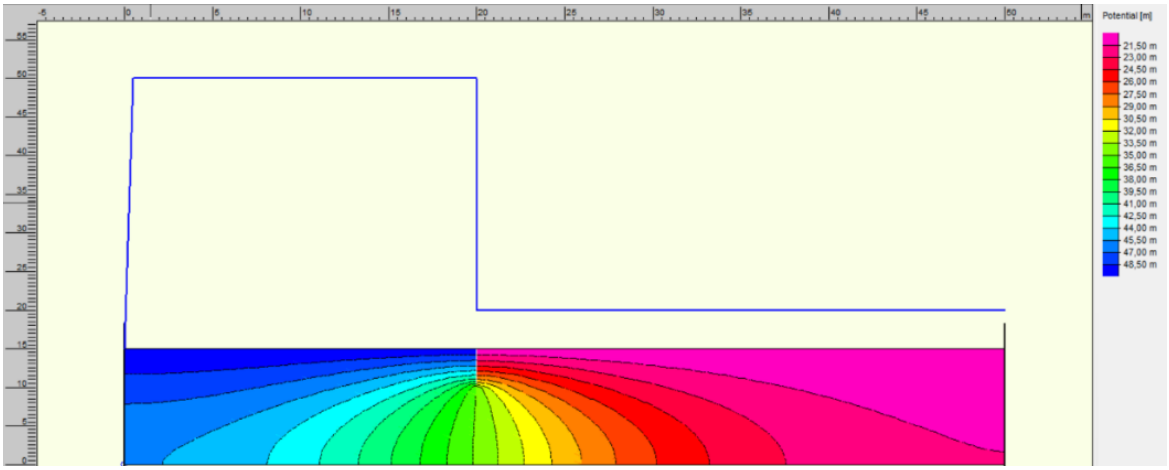

Figure 4.2: 2D Flow net of the experimental model for an upstream water level of 50 centimetres.

Depending on the calculation of the global stability criterion at the meso and macro scale, different values for the hydraulic head are used as input in the two-pressure analytical model. For the meso scale, the vertical hydraulic gradient is determined for all nodes in the defined grid. Therefore, the values of hydraulic head from Deltares MSeep model are calculated for all coordinates in the flow net corresponding to the nodes in the defined grid. On macro scale, the vertical hydraulic gradient is determined for the entire heave failure zone. Therefore, the values for the hydraulic head in the centre at the top of the heave zone and at the centre of the bottom of the heave zone are determined in the MSeep model.

4.4 Modelling a vertical top load

This study assesses the effects of a variable vertical top load on hydraulic heave failure. Therefore, in the analytical model a variable vertical top load component is added. This vertical top load is incorporated in the total vertical soil pressure in the global stability criterion. In the two-pressure analytical model, this vertical top load component is calculated based on the added vertical load on the loaded cover plate in the experimental scenarios. These experimental scenarios are further elaborated in Section 5.4. For the computation of the vertical top load, the total weight of the three small cubic water containers, acrylate cover plates and the extra water on top of the cover plate is converted to a load in kilonewton per square meter. Therefore, first the weight of the extra water on top of the cover plate is determined.

$$W_{water} = ((L_{sheet} * B_{sheet} * h_{water}) - (V_{sheet} + 3 * V_{im,cube})) * \rho_{water} \quad 4.2$$

Where,
W_{water} is the weight of the extra water on top of the loaded cover plate [kg]
L_{sheet} is the length of the loaded cover plate [m]
B_{sheet} is the width of the loaded cover plate [m]
h_{water} is the height of the water on top of the soil [m]
V_{sheet} is the volume of the acrylate sheets where the cubic water containers are placed on [m^3]
$V_{im,cube}$ is the immersed volumed of a cubic water container [m^3]
ρ_{water} is the density of water [kg/m^3]

With the weight of the extra water on top of the cover plate, now the total vertical load can be calculated.

$$\sigma_z = \frac{(3 * W_{cube} + W_{sheet} + W_{water}) * g}{1000 * L_{sheet} * B_{sheet}}$$

4.3

Where,
σ_z is the total vertical top load [kN/m^2]
W_{cube} is the total weight of cubic water container [kg]
W_{sheet} is the weight of the acrylate plates where the cubic water containers are placed on [kg]
g is the gravitational constant [= 9,81 m^2/s]

This vertical top load is the input value for the load for Equation 3.16. The result of this equation is the vertical stress increase ($\Delta\sigma_z$) which is added to the total downward soil pressure (G_d') (calculated with Equation 3.13) with one essential difference. The load of water on top of the soil is already included in the vertical top load component. Therefore, Equation 3.13 is altered into the Equation 4.4 to ensure the load of the water is not included twice.

$$G_d' = \gamma_{\text{sat}} * D_{screen} + \Delta\sigma_z$$

4.4

Where,
γ_{sat} is the unit weight of saturated soil [kN/m^3]
D_{screen} is the depth of the heave screen [m]
$\Delta\sigma_z$ is the vertical stress increase as result of Equation 3.16 with as input Equation 4.3 [kN/m^2]

4.5 Modelling the effects on the occurrence of piping

The calculation of modelled soil parameters in a finer grid within the heave zone facilitates the implementation of the effects of piping on heave failure. A pipe forming in the soil layer has a small diameter of approximately 5 mm. Therefore, the macro scale is not suitable to express the effects of piping. If the grid size at the meso scale is chosen at the approximate diameter of a pipe, the finer grid of the meso scale can be used to model the effects of piping. In this study, the effects of pipes are incorporated in the total downward soil pressure. Because of the chosen experimental design, piping occurs directly under the cover plates in the experiment. Therefore, the first top layer of nodes is estimated to be in a thin layer of water caused by piping. The vertical pressure in the second layer of nodes therefore only includes the vertical pressure of this thin layer of water on top (explained in Chapter 3.4). The total downward soil pressure in third and consecutive layers of nodes further below the surface is determined with the equations of the global stability criterion. An example of the total downward soil pressure determined in a meso scale grid is shown in Figure 4.4

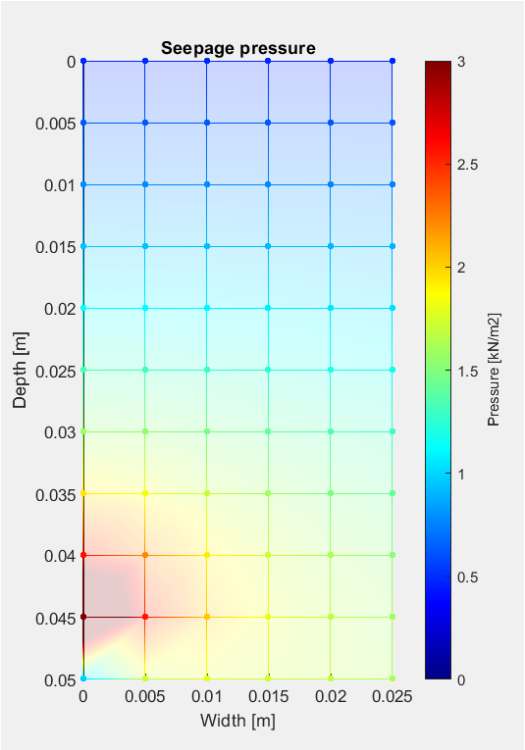

Figure 4.3: Example of seepage pressure (σ_{seep}) on meso scale

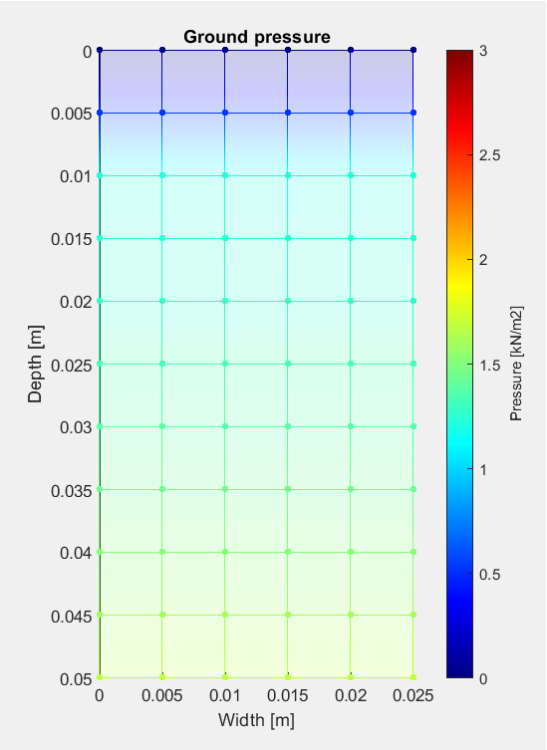

Figure 4.4: Example of soil pressure ($\sigma_{z,total}$) on meso scale

5. Experimental design of dike with heave screen

5.1 Design and lay-out of experimental model

In this experimental methodology, the research objective of the study is approached with an experimental setup. This experimental setup is constructed with the aim to represent a scaled version of a soil layer with a dike structure on top combined with a heave screen. Therefore, the experimental setup is constructed based on three main design requirements following from the research questions:

- Assessing hydraulic heave failure over a variable water height
- Assessing the effects of piping on hydraulic heave failure
- Assessing the effects of vertical loading on hydraulic heave failure

From these design requirements, subsystems in the experimental design have been defined to satisfy the three design requirements. These subsystems are listed below, and the details of their components are elaborated in the next section.

- The reference frame
- The water inlet and outlet – for a variable water height
- Cover plates – for simulating the effects of piping
- Extra vertical top load – for a variable vertical load

In this experimental setup several experiments are conducted following from determined experimental scenarios. Figure 5.1 and Figure 5.2 show a side view and 3D view of the 3D model of the experimental setup. The constructed experimental setup is presented in Figure 5.3 and Figure 5.4

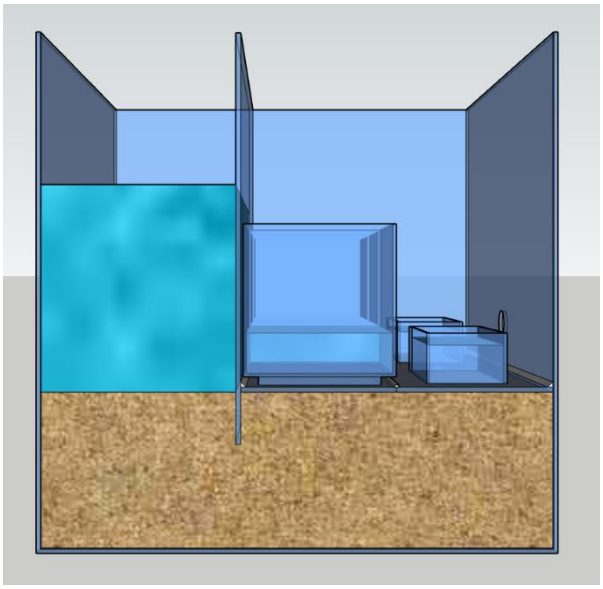

Figure 5.1: Side view of 3D experimental model

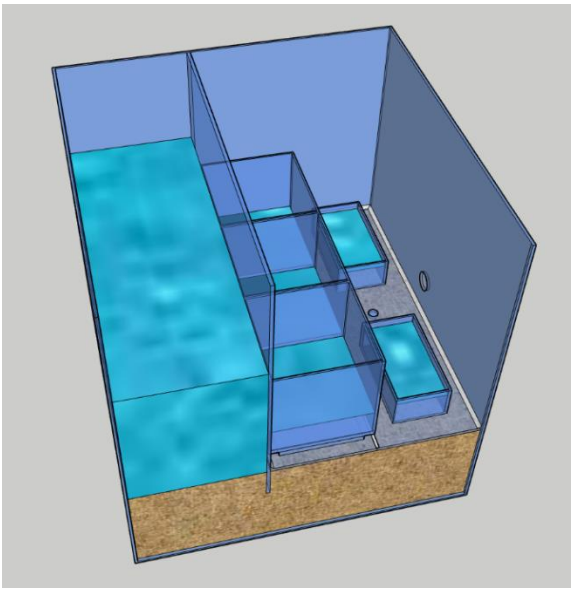

Figure 5.2: 3D view of 3D experimental model

Figure 5.3: Side view of experimental setup (after heave failure)

Figure 5.4: 3D view of experimental setup (during experiment)

5.2 Subsystems in experimental model

In the experimental setup four subsystems are defined. Each subsystem contains several components which are made from a specific material and its corresponding dimensions. For each subsystem, the details of their components are listed in the following sub-sections.

5.2.1 The reference frame

All experiments are conducted in a large transparent cubic base container. The base container is constructed from acrylate. In the bottom of this base container, the soil layer is created. All experiments are conducted with a constructed soil layer with a height of 15 centimeters. In the base container, a vertical heave screen is located. This heave screen is fixed in a slider construction at a depth of 5 centimeters into the soil layer. In this slider construction, sealant is applied to ensure a fixed depth and to prevent for leakage around the heave screen. In Figure 5.5, the side view of the cubic base container is shown with its dimensions.

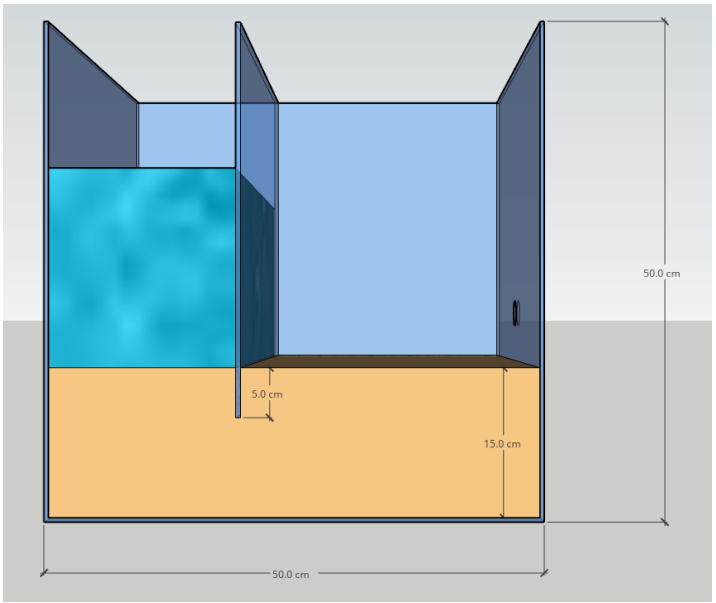

Figure 5.5: Side view cubic base container with heave screen (slider construction)

5.2.2 The water inlet and outlet

Hydraulic heave failure in the experiments is assessed under a variable, increasing water height. In the experiments it is tested at which critical upstream water level heave failure will occur (as example, the critical upstream water level in Figure 3.3 is parameter H_1). This result will later be compared to the analytical model results. To control the water inflow and outflow during the experiments, a water bucket equipped with a tap connection and hose is positioned on an elevated platform. The tap can be adjusted to allow a gradual and consistent water inflow. The water inlet construction is shown in Figure 5.6.

To establish a hydraulic gradient in the experimental setup, a water outlet is installed at a fixed height. In the experimental setup a tap connection is located at a height of 20 centimeters (5 centimeters above the soil layer). At this height, water is discharged from the experimental setup into a lower water tank. In Figure 5.7, the water outlet with lower water tank is displayed.

Figure 5.6: Water inlet with bucket and hose

Figure 5.7: Water outlet with lower water tank

5.2.3 Cover plates for piping

The progression of piping is a complex process in soil mechanics. To visualize the progression of piping and its effects on hydraulic heave failure, transparent acrylate plates are placed on top of the soil layer. Therefore, the progression of piping and the effects of piping near the critical water height for heave failure can be observed in the top part of the soil layer. The transparent plates function as impermeable cover layer. The transparent plates therefore represent the impermeable clay layer situated on top of sand dikes vulnerable for piping.

The experimental setup has two cover plates. Close to the heave screen, the cover plate functions as base plate for the extra vertical top load. Close to the outlet, the cover plate functions as exit point for piping. This exit point is accommodated through a hole in the cover plate with a diameter of 1,5 centimeter. To prevent leakage along the cover plates, a thin layer of clay is applied to the edges of the cover plates. This thin layer of clay also ensures that piping can only occur to the predetermined exit point In Figure 5.8, the top view of the two cover plates and the dimensions are shown.

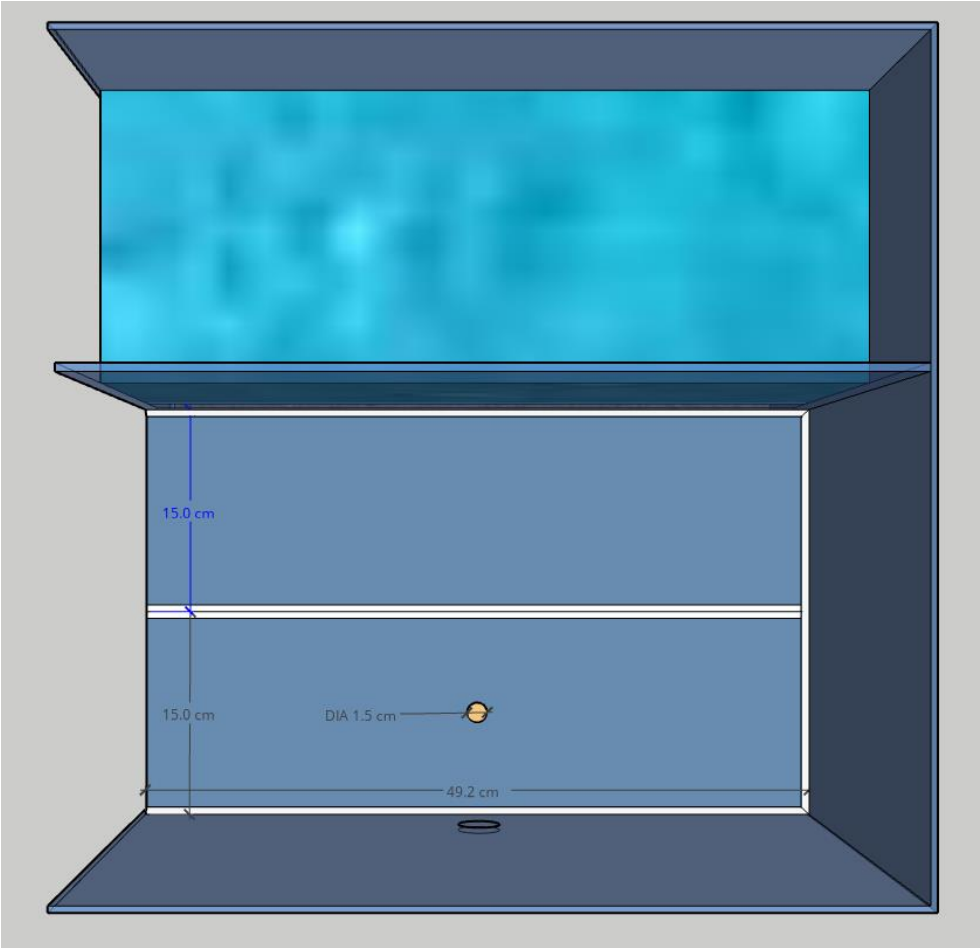

Figure 5.8: Top view cubic base container with two cover plates

5.2.4 Extra vertical top load

The experiments on hydraulic heave failure are conducted under a varying vertical top load. For a variable vertical top load in the experimental setup, small transparent acrylate cubic containers of 15 centimeters are placed on the cover plate close to the heave screen. These cubic containers can be filled with water to increase the vertical top load applied on the soil layer and thus the heave zone. On the cover plate above the heave zone, three of these cubic containers are place with each an equal weight (W_{cube}). In between the cover plate and the three cubic containers, an extra thin sheet of transparent acrylate in placed. This thin sheet ensures that the cubic containers can be positioned horizontally on the cover plate without damaging the thin clay layer placed on top of the cover plates. Each small water container is weighed to ensure that every water container has the same specific weight for the experiment.

For the experiments with an extra vertical top load, it is needed to reinforce the cover plate with exit point with extra weight. Otherwise, it would be possible that this cover plate is lifted due to water pressure before heave failure occurs. In the experimental setup, this extra weight was added with two small trays of water. In Figure 5.9, the top view of an experimental setup with extra vertical top load is shown.

Figure 5.9: Top view of cubic base container with water containers with extra load

5.3 Measurements in experimental setup

Two types of measurements are taken during the experiment. The first measurement is the critical upstream water height for which heave failure occurs. The moment of heave failure is rather sudden. Therefore, this moment of failure is filmed with a fixed smartphone. From this footage, the critical water height can be examined with an aligned ruler next to the water height. This ruler is shown in Figure 5.10.

The other measurements during the experiment concern the water potential on the side of the upstream water level. These measurements are taken with piezometers which are fixed at certain depth into the soil layer. These measurements are compared to the data from the Deltares MSeep model (explained in Chapter 4.3). Data on hydraulic head from the Deltares MSeep model were used as an input variable in the analytical two-pressure model for the computation of the hydraulic gradient. The measurements of the hydraulic head and the output of the MSeep model are compared for the validation of the use of the MSeep data in the analytical model. An example of the piezometer used in the experiment is displayed in Figure 5.11.

In addition to taking these measurements, the course of the experiment is filmed. This footage is used for analyzing the development of hydraulic pipe during the experiments and for recording the exact moment of heave failure.

Figure 5.10: Ruler for measurement of critical upstream water level

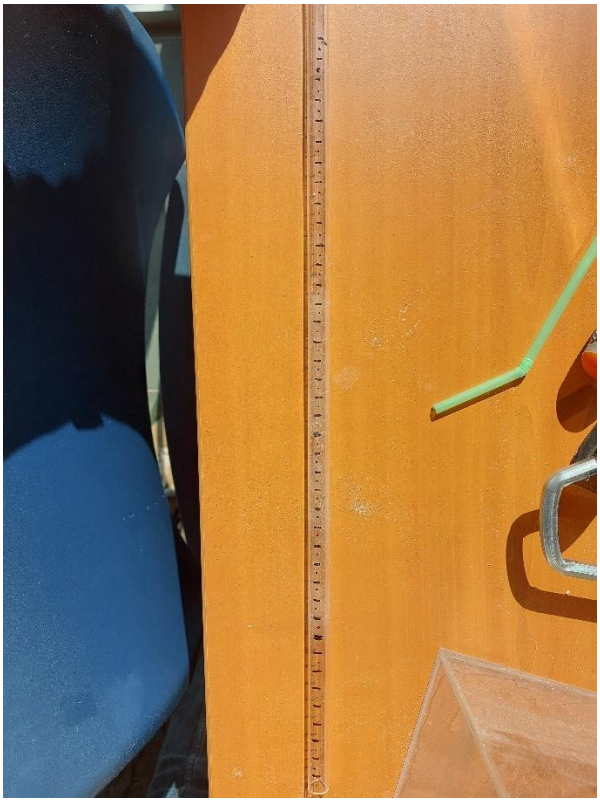

Figure 5.11: Piezometer for measurement of hydraulic head

5.4 Experimental scenarios

The experimental setup is used to perform multiple different experiments. For these different experiments, experimental scenarios have been setup. These experimental scenarios are developed in consultation with the external supervisor and following preliminary runs of the analytical two-pressure model. The experimental scenarios are listed below.

1. Standard heave experiment
2. Heave experiment with cover plates
3. Heave experiment with individual cube weight of 1,3 kg
4. Heave experiment with individual cube weight of 1,6 kg
5. Heave experiment with individual cube weight of 1,9 kg
6. Heave experiment with individual cube weight of 2,2 kg

The standard heave experiment is created as a heave experiment which is well-described by theory. This experiment is based on the existing theories for hydraulic heave failure and has a comparable setup to Figure 1.2. In the heave experiment with cover plates, the standard heave experiment is extended with the placement of cover plates with a thin layer of clay. The top view of this experimental scenario is shown in Figure 5.8. The heave experiments with added cube weights consist of the experimental setup with cover plates and three cubes loaded with a specific individual weight. This experimental scenario is shown in Figure 5.9.

The creation of the experimental scenarios in the experimental model is done using a step-by-step plan for the simulation of each scenario. This plan is summarized in steps below.

1. Compact the soil layer to a layer thickness of 15 centimetres
2. Fully saturate the soil layer and smooth out the top of the soil layer
3. Place piezometers at set locations and setup the camera's
4. Place cover plates with a thin layer of clay (depending on scenario)
5. Place three cubes with determined weight and place the extra weights (depending on scenario)
6. Measure the height of the soil layer and the depths of piezometers as check

5.5 Soil characteristics of the experimental model

The modelling of the local and global stability criterion is based on soil-mechanical equations. These equations are based on several soil characteristics. The two-pressure analytical model is created to compare analytical results to an experimental model. Therefore, the variables in the model should be comparable to soil characteristics of the soil used in the experimental design. In the local and global stability criterion, the following soil characteristics can be distinguished.

- The unit weight of the saturated soil (γ_{sat})
- The porosity of the soil (n)
- The intrinsic permeability of the soil (k_z)
- The minimum soil particle diameter in the soil ($d_{min,\ particle}$)

For the determination of these soil characteristics, three standardized laboratory tests are performed on soil samples of the experimental design. These are a soil proctor test, a soil permeability test and a soil sieving test. These tests are performed in an accredited laboratory of Fugro. The soil proctor test determines the maximum dry density of the soil sample. Together with the maximum dry density and the density of soil particles, the porosity of the soil can be calculated. This is shown in Equation 5.1.

$$n = 1 - \frac{\rho_{dry}}{\rho_s} \tag{5.1}$$

Where,
n is the porosity of the soil [-]
ρ_{dry} is the dry density of the soil [kg/m^3]
ρ_s is the soil particle density [=2650 kg/m^3 (Verruijt, 2001)]

The known porosity of the soil sample makes it possible to determine the unit weight of saturated soil. Therefore, Equation 5.2 is used.

$$\gamma_{sat} = (\rho_{dry} * f_\rho) + n * \gamma_w \tag{5.2}$$

Where,
f_ρ is the conversion factor for density to volumetric force [=0,00981 m/s^2]

The soil permeability test directly determines the permeability of the soil and therefore the value for k_z. The soil sieving test determines the particle size distribution of the soil sample. From this particle size distribution, the minimum soil particle diameter can be determined. This is defined as the soil

particle diameter of the smallest 1% of soil particles present in the soil sample. The results of the laboratory test are shown in Table 5.1. The detailed lab reports of the three tests from Fugro can be found back in Appendix B.

Table 5.1: Laboratory results on the soil characteristic of the soil sample

Laboratory test	Soil characteristic	Laboratory result
Soil proctor test	The maximum dry density (ρ_{dry})	1599 kg/m^3
Soil permeability test	The permeability of the soil (k_z)	1,7E-04 m/s
Soil sieving test	The minimum soil particle diameter in the soil ($d_{min,\ particle}$)	0,063 mm

6. Experimental & analytical results

6.1 Hydraulic heave failure mechanism

Hydraulic heave can occur through the instability of a soil particle (local heave failure) or the instability of the entire heave failure zone (global heave failure). During the experiments, moment of failure of hydraulic heave have closely been observed. From observations, video footage of the moment of failure and discussions with the external supervisor, the moment of failure could be summarized as an outburst of soil aggregate. First, upstream deformation of the soil layer occurred, followed by the outburst of a soil aggregate. In Figure 6.1, upstream deformation of the soil layer in the standard heave experiment is shown. In this picture can be seen that a stretch of the soil close to the heave screen is subsided. The moment of the soil aggregate outburst is depicted in Figure 6.2. This picture shows the beginning of the displacement of the cover plates and a large outflow of soil particle at the exit point. In the experiments with extra vertical loading, the leaching of soil grains is observed. This leaching of soil grains is only observed near formed hydraulic pipes.

Figure 6.1: Top view of soil deformation in standard heave experiment

Figure 6.2: Top view of the moment of the soil aggregate outburst in heave experiment 6 (2,2 kg)

The analytical two-pressure model determines the critical soil particle diameter. If the minimum soil particle diameter in the soil is smaller than the critical soil particle diameter, local heave can occur. The results on both soil particle diameters are shown in Table 6.1. Since the minimum soil particle diameter in the experiments is greater than the critical soil particle diameter, the occurring heave failure mechanism will be global heave failure. This is in line with the observations presented above.

Table 6.1: Soil particle diameters with corresponding analytical heave failure mechanism

Critical soil particle diameter	Minimum soil particle diameter	Resulting analytical heave mechanism
32,30 µm	63,00 µm	Global heave failure mechanism

6.2 Critical upstream water height

Hydraulic heave failure occurs at a critical upstream water height. This critical upstream water height is defined as the measurable moment of hydraulic heave failure. The results for the critical upstream water height in the experimental setup and the analytical macro scale model are shown in Table 6.2. This table shows the critical upstream water heights for all experimental scenarios and the corresponding analytical results of the two-pressure model. The analytical solution on critical upstream water height for the standard heave experiment is determined based on the critical hydraulic gradient and the two-pressure model. The results of both computations were identical. The experimental results are divided into two categories. The upstream water height for which soil deformation took place and the upstream water height for which heave failure occurred.

Table 6.2: Critical upstream water height for experimental scenarios

	Experimental - deformation	Experimental - failure	Analytical
Standard heave experiment	33,3 cm	37,2 cm	35,1 cm
Heave experiment 2 (cover plates)	35,9 cm	38,4 cm	35,4 cm
Heave experiment 3 (1,3 kg)	44,0 cm	44,5 cm	39,5 cm
Heave experiment 4 (1,6 kg)	46,2 cm	46,4 cm	43,2 cm
Heave experiment 5 (1,9 kg)	44,5 cm	45,4 cm	46,6 cm
Heave experiment 6 (2,2 kg)	45,8 cm	46,1 cm	50,0 cm

These results are plotted in Figure 6.3. In this figure, the critical water heights are plotted with respect to the applied vertical loading on top of the soil. In the figure, the linear trend of the experimental results of deformation and failure is shown with a regression line. This regression line is determined for the experiments where cover plates were applied (experimental scenarios 2 till 5).

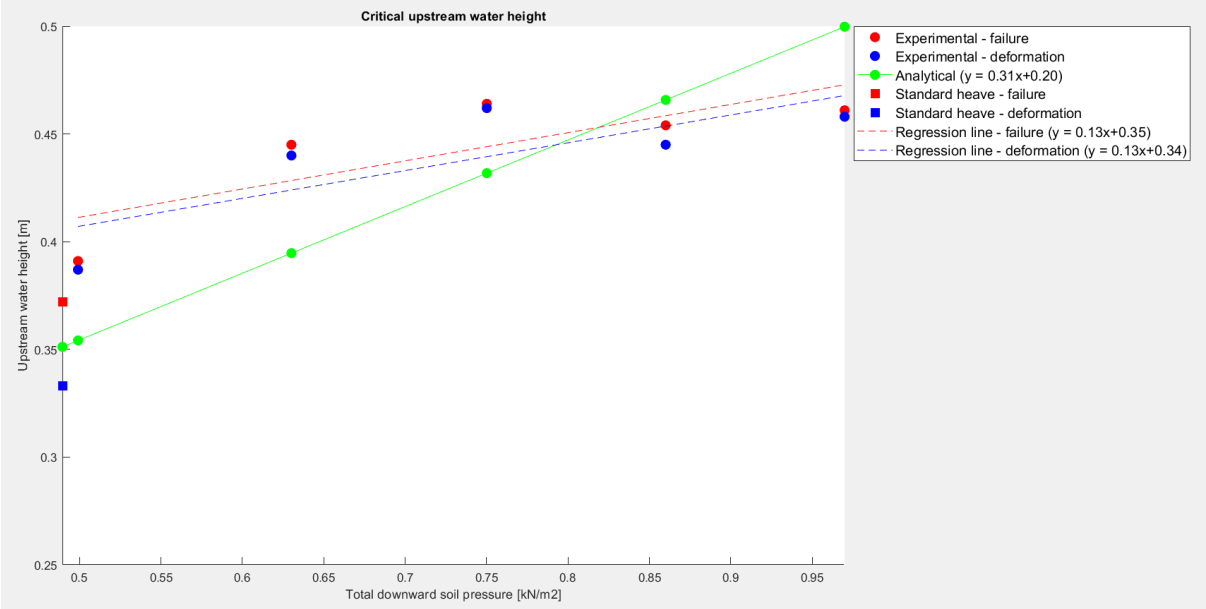

Figure 6.3: Critical upstream water height at applied vertical load

In Figure 6.3, the results of the standard heave experiment are plotted separately from the other experiments due to the absence of cover plates in this experiment. There could be noticed that there

are two phases in the experimental and analytical results of the other experiments. In heave experiment 2, 3 and 4, the analytical model consistently underestimates the critical water height. In heave experiment 5 and 6, the analytical model overestimates the critical water height.

The strength of the linear trend of the experimental results is shown by the coefficient of determination (R^2). This coefficient is a measure of the goodness of fit of the results to the regression line. The linear trend shown by the regression lines can be compared to the linear relationship of the model. Therefore, the directional coefficients are compared to each other. In these results, the directional coefficient indicates the magnitude of the linear effect between soil pressure and critical upstream water height. The coefficient of determination and the directional coefficient of the results are shown in Table 6.3.

Table 6.3: Statistics of experimental and analytical results.

	Coefficient of determination (R^2)	Directional coefficient
Experimental – failure	0,65	0,13
Experimental – deformation	0,63	0,13
Analytical	1,00	0,31

6.3 Effects of occurrence of piping on heave

In the experiments where the cover plates are applied, the aim was to recreate the occurrence of piping. In the experiments with an applied extra vertical load by the cubic water containers, the recreation of piping succeeded. The start of the occurrence of piping could be observed in general around an upstream water height of 18,5 centimetres. During the experiment, the piping process intensified. The intensity and development of piping differed in each heave experiment but in general 4 stages can be determined in the piping process in the experiments. These stages are shown in Figure 6.4 till Figure 6.7. These figures represent a schematization of the top view of the downstream side of the experimental setup with two cover plates and the heave screen.

In the first stage, a single pipe was forming in direction of the centre of the heave screen. In the second stage, multiple pipes were forming. During this stage, these extra pipes were sometimes forming alternately. In the third stage, pipes were forming towards other pipes. This created a network of pipes. In this stage, the pipes formed towards heave screen expanded in width. In the fourth stage, one large pipe expanded in width. This caused the network of pipes to transform into a wide pipe. After this stage, upstream soil deformation occurred in similar size of the width of the pipe downstream. The soil deformation was quickly followed by the moment of hydraulic heave failure. At the moment of failure, an outburst of a soil aggregate pushing the cover plates upwards was observed.

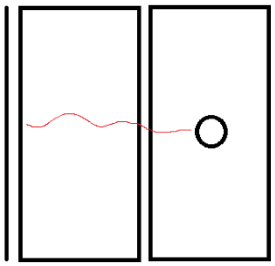

Figure 6.4: General progression of piping (stage 1)

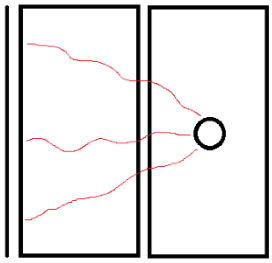

Figure 6.5: General progression of piping (stage 2)

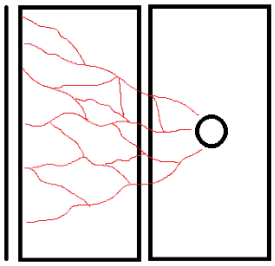

Figure 6.6: General progression of piping (stage 3)

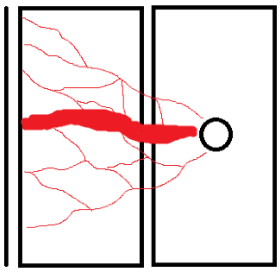

Figure 6.7: General progression of piping (stage 4)

For the analytical analysis of the effects of the occurrence of piping, experiment 5 with an extra applied vertical load (1,9 kg) was elaborated. For this experiment, the total seepage pressure, total downward soil pressure and excess seepage pressure were determined on meso scale. The resulting grid is visualised in Figure 6.8.

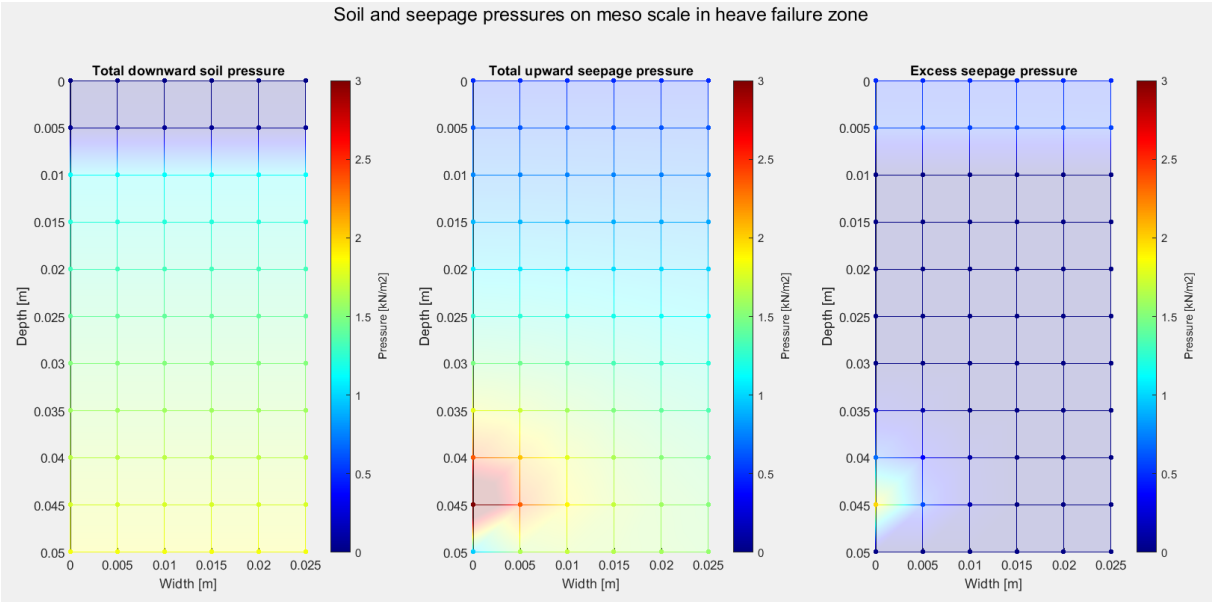

Figure 6.8: Soil and seepage pressure on meso scale for heave experiment 5 (1,9 kg)

For this heave experiment also the factor of safety has been determined on meso scale. This factor of safety for all nodes are shown Figure 6.9.

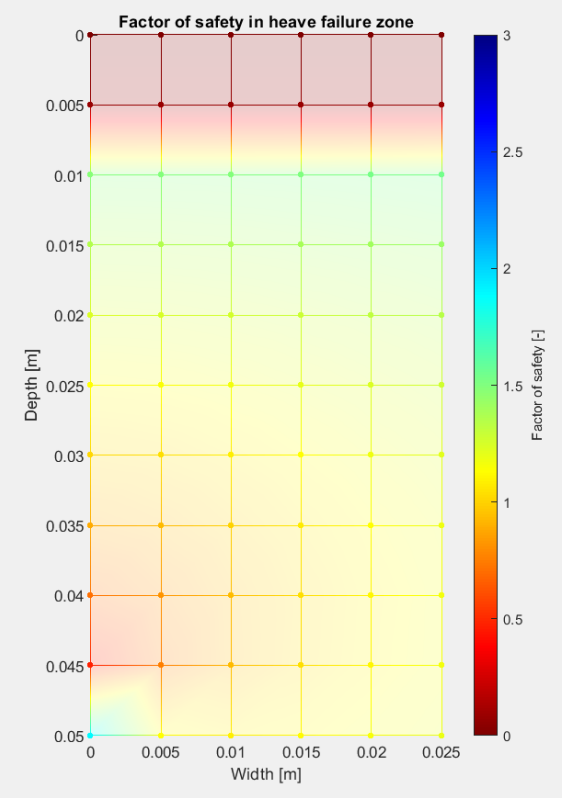

Figure 6.9: Factor of safety on meso scale for heave experiment 5 (1,9 kg)

In results of the factor of safety depicted in Figure 6.9 can be seen that especially the location of the pipe in the top layer of the nodes has a very low factor of safety. Also, near the bottom of the heave screen, a node with a low value of the factor of safety is shown. This low factor of safety for this node is caused by the high seepage pressure for this node shown in Figure 6.8 . At the location of the pipe, the total downward soil pressure is low due to formed pipe. The values of the factor of safety on meso scale can be compared to the factor of safety computed on macro scale, excluding the effects of piping. The three values of the factor of safety are shown in Table 6.4.

Table 6.4: Macro and meso factor of safety – heave experiment 5

Macro factor of safety	Meso factor of safety (bottom heave screen)	Meso factor of safety (pipe location)
1,00	0,47	0,08

6.4 Hydraulic head measurements

In the heave experiments, the hydraulic head was measured at the upstream side of the experimental setup. This hydraulic head was measured with four piezometers at several upstream water heights. These measurements were taken to compare to the hydraulic head computation in Deltares MSeep. In the last three experiments, the measurements on hydraulic head were taken at the same locations at same depths of 5 cm and 10 cm in the experimental setup. These locations and depths are shown in Figure 6.10.

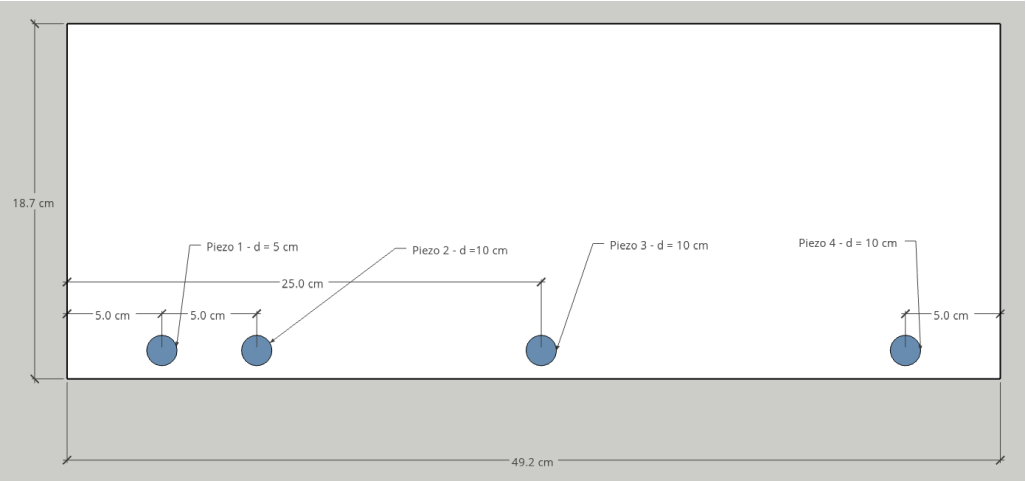

Figure 6.10: Location of piezometer on upstream side of the experimental setup (the variable *d* is the measuring depth)

These measurements of the last three experiments are plotted together with the results of the Deltares MSeep model for the corresponding upstream water height. For the measurements of the piezometers, a regression line is plotted for the two measurement depths. This plot is shown in Figure 6.11.

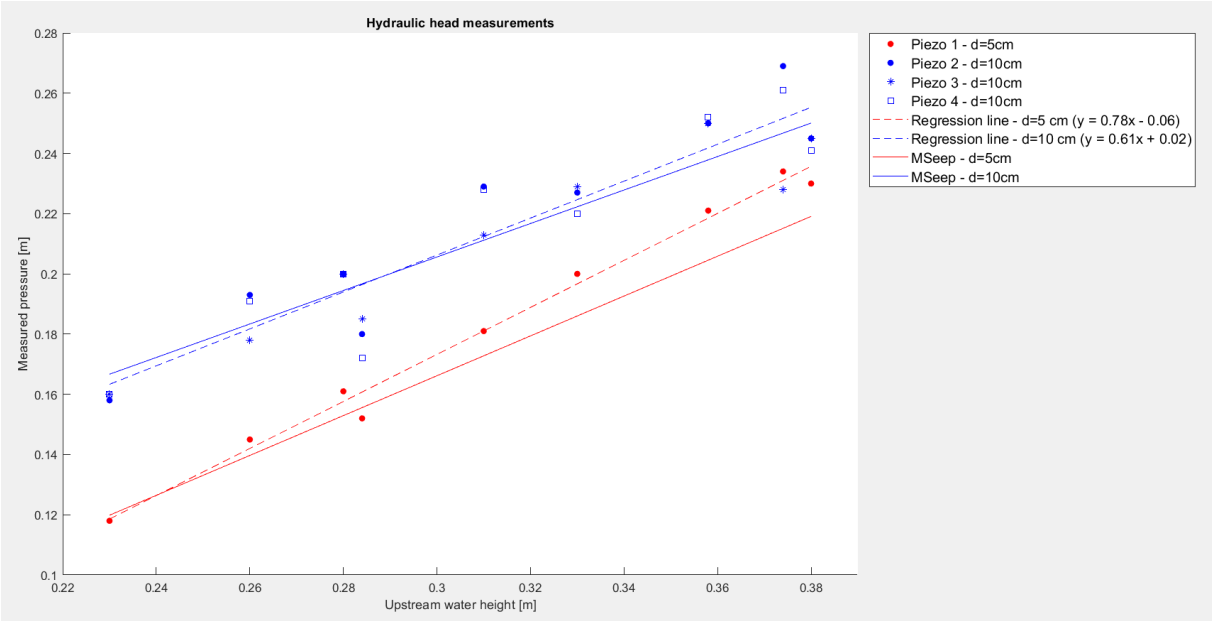

Figure 6.11: Hydraulic head measurements from piezometers and MSeep

The goodness of fit of the measurement results is shown with the coefficient of determination (R^2). Therefore, this coefficient is computed for the results of the four piezometers. Results are shown in Table 6.5.

Table 6.5: Coefficient of determination for the results of the piezometers

	Piezo 1	Piezo 2	Piezo 3	Piezo 4
Coefficient of determination (R^2)	0,99	0,90	0,90	0,86

7. Discussion

7.1 Implications on incorporating the effects of vertical loading and piping in the hydraulic heave mechanism

In this study, three levels of details are used in the assessment on hydraulic heave failure. The micro and macro scale are in literature described methods for assessment of local and global heave failure. The meso scale extends the theory on global heave failure to heave failure on a smaller scale. This gives a more comprehensive understanding of the heave process inside the heave zone. The analytical model shows that on meso scale, the critical point for heave failure is reached at specific locations before the critical point for heave failure is reached on macro scale. This indicates that at specific locations in the heave zone, heave failure could already occur before macro scale heave failure occurs. In the comparison of the experimental results and analytical results, the analytical model on macro scale for experiment 5 and 6 overestimates the critical point of failure. The analytical model on meso scale indicates an earlier point of failure. However, since the analytical model on macro scale underestimates the critical point of failure for experiment 2, 3 and 4, the computed meso scale cannot directly be presented as the solution. Also, the computation of the hydraulic heave failure on meso scale includes flaws in the incorporation of the piping mechanism in two-pressure model.

The effects of the occurrence of piping are in the analytical two-pressure model implemented in the total downward soil pressure. However, the effects of the occurrence of piping are not included in the total seepage pressure. The reason here for is the complexity of the piping process. The intensity and development of the piping process is dependent on the upstream water height and differs for every heave experiment. The effects of the occurrence of piping on heave is therefore difficult to express in an analytical equation. A numerical finite element model could give new insights for a further detailed implementation of the effects of the occurrence of piping on soil and seepage pressure. This development of a numerical model is however outside the scope of this research project.

In the analytical results, the effects of vertical loading are visible in a clear linear relationship. In the experimental results, a linear correlation could be found. The strength of this linear correlation is stated by the coefficient of determination. This coefficient implies a weak linear correlation. For the effects of vertical loading also the directional coefficients of analytical and experimental results can be compared. Here, the analytical results compared to the experimental results show a higher directional coefficient. This indicates that the analytical model computes a larger effect of vertical loading on heave failure then is observed in the experimental results. Therefore, the analytical model consistently overestimates the quantification of the effect of the vertical load on heave failure.

In the experimental and analytical results, a division is shown between comparison of heave experiment 2, 3 and 4 and comparison of heave experiment 5 and 6. In the first part, the analytical model consistently underestimated the failure point. In the second part, the model overestimates the failure point. In the clarification of these results, one factor was found which indicated to be crucial. This crucial factor is the width of pipe in stage 4 (depicted in Figure 6.7). In the video footage of heave experiment 5 and 6 was observed that the width of the pipe was significantly wider than in experiment 2, 3 and 4. This implies that the piping mechanism is directly connected to the heave failure mechanism. An article of van Beek, shows that the piping width is directly related to the hydraulic head (Van Beek et al., 2022). Interpretating this article together with the implication followed from the experiments, there can be stated that piping and heave failure directly affect each other. Because both

hydraulic heave failure and piping failure are dependent on the critical upstream water height. To conclude, more research into the connection between piping and heave failure is essential for further incorporation of the effects of piping on hydraulic heave.

In the experimental results, two steps of the heave failure process are described. Namely, deformation and failure. This was unexpected since the theoretical framework only describes heave failure as a one-step process. These two steps in the heave failure process seems logical due to interaction of the seepage and soil pressure. At the moment of deformation, part of the soil layer is pushed towards the downstream side of the heave screen. This creates an increased soil pressure. The seepage and soil pressure therefore find a new equilibrium condition. The effect of the two steps is mainly visible in the standard heave experiment. Therefore, in the assessment of the experimental results of the heave experiments with an extra vertical load, the distinguishment of these two steps does not seem to be crucial. The experimental results of the article of Tanaka and Verruijt also show the moment of soil deformation and the moment of actual heave failure. However, the article concludes that theory for the behaviour of the sand between the moment of deformation and the moment of heave failure still needs to be developed (Tanaka & Verruijt, 1999).

7.2 Potential deficiencies in the experimental and analytical model

The objective of the analytical two-pressure model is to compare it to the experimental model. In comparison, the extended theory on heave failure in analytical model is validated with experimental results. However, several main differences between the analytical model and experimental design can be noted. The analytical two-pressure model is two-dimensional representation of the heave failure zone in a soil layer. The experimental model represents a three-dimensional representation of the heave failure zone. Hydraulic head measurements in the experimental model (shown in Figure 6.11) have been taken to examine the three-dimensional effect on seepage flow and conclude if Deltares MSeep is a suitable for the modelling of hydraulic head in the analytical model.

In the comparison of the plotted regression lines and the MSeep model, the resemblance between the regression lines and the MSeep model seems well. The analysis on the coefficients of determination of all piezometers show coefficients close to 1. This means that the measurements closely related to the plotted regression lines. Therefore, the Deltares MSeep model closely matches with the measurements in the experimental setup. Therefore, the three-dimensional effect in the experimental setup is neglectable and does not consistently influence the hydraulic head in the width in the experimental setup.

The analytical model has been developed with the intention to model the two main pressures that can cause heave failure according to existing theories on heave failure. In the theoretical framework, the theories of Terzaghi, Garai and Das & Soban on hydraulic heave failure are elaborated. After, the conducted experiments, the article of Tanaka & Verruijt was examined on the mechanism of seepage failure. This article described a new computation method of heave failure. This method is mentioned as “prismatic failure with friction”. The computation method considering the frictional forces on the sides of the heave zone (Tanaka & Verruijt, 1999). This new computational method with friction suggests that the standard two-pressure model underestimates the moment of hydraulic heave failure. This trend can be observed in the analytical results in Figure 6.3. However, there could also be observed that this trend of underestimation is not consistently. Therefore, it is doubtful if these friction forces have a significant influence on heave failure.

The compaction of the soil layer is an essential factor in the experiments. The compaction of the soil layer directly influences the density of the soil in the heave zone and the development of piping in the experiments. Therefore, the moment of heave failure and effects of the occurrence of piping on heave failure is affected by the compaction of the soil layer. The compaction of the soil in the experiments is done manually as accurate as possible but can differ between the experiments.

The experimental model represents a scale version of a heave screen with a dike structure on top. One experimental part unintendedly influences the heave process. This experimental part is the thin clay layer which is applied on top of the cover plates. This main function of this thin clay layer is to ensure that there is no leakage at the edges of the cover plates. However, this thin layer of clay also gives extra vertical strength to the cover plates. The effect of this extra strength is difficult to estimate. Therefore, the implementation of this extra strength is not considered in the analytical two-pressure model.

8. Conclusion & recommendations

How can existing analytical equations on heave failure be used to consider the effects of dike structures with heave screens on heave failure?

The results of the analytical two-pressure model show a clear linear correlation between the critical upstream water height and the applied vertical load on top of the soil. Therefore, it can be concluded that following to analytical two-pressure model the vertical top load has a positive, linearly correlated effect on the critical upstream water height and thus the critical point for heave failure.

In the analytical model, occurrence of piping is modelled in the total downward soil pressure. The effects of the occurrence of piping are analysed on meso scale. This analysis on meso scale shows a lower critical point of failure on specific locations in the heave zone then in the analysis on macro scale. However, the inconsistency in the experimental results and the uncertainty in the connection of piping and heave failure indicates that there cannot be made a concrete conclusion on the effects of the occurrence of piping on the critical point of heave failure. What can be concluded is that the pipe width is related to the critical point of heave failure.

The analytical results on the resulting hydraulic heave failure mechanism show that the decisive heave mechanism is global heave failure. This is in line with observations from the experiments. Therefore, the conclusion can be made that heave failure occurs through the global heave failure mechanism. For the global heave failure mechanism, a distinction is made between meso scale and macro scale. The macro scale analysis is substantiated by literature. This meso scale analysis on hydraulic heave failure is introduced in this study. The meso analysis shows critical failure points in the heave zone before heave failure at macro scale. For a conclusion on the decisive meso or macro scale for heave failure, more research into the incorporation of the effects of the occurrence of piping on heave failure is needed.

How do trends in experimental results of heave failure at dike structures with heave screens compare to predictions following from existing analytical solutions?

In all experiments performed in the experimental setup, two critical thresholds could be observed. These were the threshold of soil deformation and the threshold of hydraulic heave. Both thresholds generally occurred at increasing upstream water heights for increasing vertical loads.

Two experimental and analytical variables can be compared. These are the critical upstream water height and the hydraulic head. In the analytical two-pressure model, a clear positive linear correlation is shown between the critical upstream water height and the applied vertical load. The experimental results on the critical upstream water height show a weak positive linear correlation. From the comparison on the linear correlations can be concluded that from the presented results, an increased vertical top load results in an increased critical upstream water height with a linear relationship. However, for the quantification of the effect of vertical loading on heave failure, it is desirable to perform more experiments with an increased vertical top to further study the correlation between the critical upstream water height and the applied vertical top load. From the comparison of the hydraulic head can be concluded that there is no significant structural deviation of a piezometer which shows a significant three-dimensional effect in the experimental setup. Therefore, Deltares MSeep is a suitable for modelling the hydraulic head in the analytical two-pressure model.

8.1 Recommendations for future research and the design criterium

From the results of this study multiple recommendations can be made for further research. A crucial topic following from this study is the connection between the failure mechanisms piping and heave failure. This topic is an interesting opportunity for further experimental research but also numerical research. The connection between both mechanisms is analytically difficult for further research. The development of numerical finite element models could provide new insights in the connection between both failure mechanism. The current experimental model gives the possibility for further investigation. An interesting experiment would be to test occurrence of hydraulic heave failure at a constant water level below the critical upstream water level. If hydraulic heave occurs at lower water level than the critical upstream water height, the hydraulic heave failure mechanism could be related to the occurrence piping. This research could potentially shed a new light a combined approach of assessing piping and heave failure at heave screens.

The current heave design criterium defined by Deltares determines the critical point for heave failure using the critical hydraulic gradient. This calculation method is not suitable for the incorporation of a vertical load. The two-pressure calculation model is suitable for the incorporation of a vertical load. Therefore, it is recommended to further investigate the two-pressure calculation model with experimental research. This could lead to the renewal of the heave design criterium which can incorporate the effect of the vertical load caused by a dike structure on heave failure.

9. References

Boussinesq, J. (1883). Application des Potentials a L'Etude de L'Equilibre et du Mouvement des Solides Elastiques. Gauthier-Villars.

Cistin, J. (1966). Seepage Hydraulics - A Contribution to the Problem of Inner Suffusion of Non-cohesive Layers.

Darcy, H. (1856). Les fontaines publiques de la Ville de Dijon. Dalmont.

Das, B. M., & Sobhan, K. (2013). Principles of Geotechnical Engineering, SI Edition. Cengage Learning.

Förster, U., Van den Ham, G., Calle, E., & Kruse, G. (2012). Onderzoeksrapport Zandmeevoerende Wellen. Deltares.

Garai, J. (2016). Hydraulic failure by heave and piping. https://doi.org/10.1201/9781315375045-52

Hoogwaterbeschermingsprogramma. (2017). Waterveiligheidsportaal. https://waterveiligheidsportaal.nl/#!/nss/nss/current

Kovks, G. (1981). Chapter 3.2 The motion of grains in cohesionless loose clastic sediments. In Developments in water science (Vol. 10, pp. 349–379). Elsevier BV. https://doi.org/10.1016/s0167-5648(08)70045-5

Oldhoff, R. (2013). Meetkwantiteit versus toetsingskwaliteit: Onderzoek naar de invloed van informatiedichtheid op het toetsresultaat van de rekenregel van Sellmeijer voor de toetsing op piping. Universiteit Twente.

Quanyi, X., Liu, J., Han, B., Li, H., Li, Y., & Xuanzheng, L. (2018). Critical Hydraulic Gradient of Internal Erosion at the Soil–Structure Interface. Processes, 6(7), 92. https://doi.org/10.3390/pr6070092

Tanaka, T., & Verruijt, A. (1999). Seepage Failure of Sand Behind Sheet Piles—The Mechanism and Practical Approach to Analyze—. Soils and Foundations, 39(3), 27–35. https://doi.org/10.3208/sandf.39.3_27

Terzaghi, K. (1922). Der Grundbruch an Stauwerken und seine Verhutung (The failure of dams by piping and its prevention). (Vol. 17). Die Wasserkraft.

Van Beek, V., Robbins, B. A., Rosenbrand, E., & Van Esch, J. (2022). 3D modelling of backward erosion piping experiments. *Geomechanics for Energy and the Environment*, *31*, 100375. https://doi.org/10.1016/j.gete.2022.100375

Verruijt, A. (2001). Grondmechanica. TU Delft.

Wiggers, A., Sanders, M., Niemeijer, H., & Tonneijck, M. (2022). POV PipingPortaal. POV Piping.

Wudtke, R. B. (2008). Failure Mechanisms of Hydraulic Heave at Excavations. 19th European Young Geotechnical Engineers' Conference.

Appendix A

Analytical two-pressure model code in MATLAB

A.1 MATLAB code for heave computation at constant water level

```
clear all, clc
%% Heave analytical solution for constant water height %%
%% Model settings
dike_load = 1;       % method for vertical loading, 1 = standard heave, 2 = heave with
cover plates
discr_terzaghi = 1;  % discretization of terzaghi failure zone, 0 = off, 1 = on
%% Input variables
d_particle = 63;      %[um] (smallest 1% of soil particle size in micrometer)
y_dry = 15.68;        %[kN/m3] (max unit weight of dry soil)

W_cube = 1.9;         %[kg] (Weight of cube) eff_water height resp: 1.3 2.8 4.3 5,8 cm

phi_high = 0.20;      %[m] (upside potential heave screen MSeep (xcoor = ~0.215 ycoor =
0.15)
phi_low = 0.28778;    %[m] (downside potential heave screen MSeep (xcoor = ~0.215 ycoor =
0.10)
%% Parameters
% soil equation parameters
h_ground = 0.15;                %[m] (height soil layer)
d_hscreen = 0.05;               %[m] (depth heave screen)
g = 9.81;                       %[m2/s] (gravity constant)
y_w = 9.789;                    %[kN/m3] (unit weight water)
y_s = 25.99;                    %[kN/m3] (unit weight of soil particles) - 2650 kg/m3
k_z = 1.7e-04;                  %[m/s] (permeability of the soil)
mu_visc = 0.0012;               %[kg/ms] (viscosity of water) (literatuur!)
n_por = 1-(y_dry/y_s);          %[-] (porosity percentage
y_sat = y_dry+n_por*y_w;        %[kN/m3] (unit weight of saturated soil)
rho_s = y_sat*101.971621;       %[kg/m3] (literatuur!)
rho_w = y_w*101.971621;         %[kg/m3] (literatuur!)
i_crit = (y_sat-y_w)/y_w;       %[-] (critical hydraulic gradient based on saturated soil)
%y_eff = (1-n_por)*(y_s-y_w);   %[-] (effective unit weight soil based on porosity)
%i_crit = y_eff/y_w; %critical  %[-] (critical hydraulic gradient on porosity)
phi_txt = load("phi_txt_19.txt");  %input from MSeep

% vertical stress parameters
L_dike = 0.492;                 %[m] (length bottom sheet dike)
B_dike = 0.15;                  %[m] (width bottom sheet dike)
d_dike = 0.005;                 %[m] (thickness sheet)
L_cube = 0.15;                  %[m] (length dike cube)
Lb_cube = 0.144;                %[m] (innerlength dike cube)
Hb_cube = 0.147;                %[m] (innerheight dike cube)
rho_plexi = 1190;               %[kg/m3] (density plexi)

L_tsheet = 0.45;                %[m] (length thin sheet)
B_tsheet = 0.12;                %[m] (width thin sheet)
d_tsheet = 0.004;               %[m] (thickness thin sheet)

%% Determination of volumes, weights & loads of dike structure
h_imm_cube = phi_high-(h_ground+d_dike+2*d_tsheet);          %[m] (immersed depth of
cube)

Tot_V_dike = L_dike*B_dike*(phi_high-h_ground);              %[m3] (filled volume above
loaded cover plate)
V_bsheet = L_dike*B_dike*d_dike;                            %[m3] (volume of plexi base
sheet)
V_esheet = 2*L_tsheet*B_tsheet*d_tsheet;                    %[m3] (volume of plexi extra
sheet)
```

```
V_cube = L_cube^2*h_imm_cube;                                   %[m3] (immersed volume of
cube
V_water_w13 = Tot_V_dike-(V_bsheet+3*V_cube);                   %[m3] (water volume in
w_cube 1.3 kg exp -> "gele doekjes")
V_water_oth = Tot_V_dike-(V_bsheet+V_esheet+3*V_cube);          %[m3] (water volume in other
exp)

Tot_M_w13 = V_water_w13*rho_w + V_bsheet*rho_plexi + 3*W_cube;              %[kg] (total
mass of filled volume above loaded cover plate for 1.3 kg)
Tot_M_oth = V_water_oth*rho_w + (V_bsheet+V_esheet)*rho_plexi + 3*W_cube;  %[kg] (total
mass of filled volume above loaded cover plate other)

q_dike_w13 = ((Tot_M_w13*g)/1000)/(L_dike*B_dike);              %[kN/m2] (vertical stress of
loaded cover plate 1.3kg)
q_dike_oth = ((Tot_M_oth*g)/1000)/(L_dike*B_dike);              %[kN/m2] (vertical stress of
loaded cover plate other)
%% Local heave mechanism
% Calculating critical soil diameter
d_crit = sqrt(i_crit/((n_por*(rho_s-rho_w)*g)/(36*k_z*mu_visc)))*1000000; %[um] (critical
particle size diameter)
if d_particle < d_crit
    disp("Local stability condition")
else
    disp("Global stability condition")
end
%% Original global heave mechanism
%Global stability condition hydraulic gradient
i_ver = (phi_low-phi_high)/d_hscreen;                           %[-] vertical hydraulic
gradient
if i_ver > i_crit
    disp("critical hydraulic gradient exceeded")
else
    disp("hydraulic gradient within critical treshold")
end

%Global stability condition Sd - Gd
%Saturated soil stress in heave zone
Sig_w = y_w*(phi_high-h_ground);                                 %[kN/m2] Water pressure above
soil
Sig_s = y_sat*d_hscreen;                                        %[kN/m2] Saturated soil
pressure
G_d = Sig_s+Sig_w;                                               %[kN/m2] Total vertical soil
pressure

%Seepage pressure in heave zone
Sig_sp = y_w*i_ver*d_hscreen;                                   %[kN/m2] Upward seepage
pressure
Sig_u = y_w*(d_hscreen+(phi_high-h_ground));                    %[kN/m2] Pore water pressure
S_d = Sig_sp+Sig_u;                                             %[kN/m2] Seepage pressure
FS_heave = G_d/S_d;                                             %[-] factor of safety
%% Improved global heave mechanism
m_1_i = L_dike/(B_dike);
n_1_i = (d_hscreen)/((B_dike)/2);
I_4_1_i = (m_1_i*n_1_i)/sqrt(1+m_1_i^2+n_1_i^2);
I_4_2_i = (1+m_1_i^2+2*n_1_i^2)/((1+n_1_i^2)*(m_1_i^2+n_1_i^2));
I_4_3_i = asin(m_1_i/(sqrt(m_1_i^2+n_1_i^2)*sqrt(1+n_1_i^2)));
I_4_i = (2/pi)*(I_4_1_i*I_4_2_i+I_4_3_i);                              %vertical stress
increase component

if W_cube == 1.3
```

```
    q_inc_i = q_dike_w13*I_4_i;                                    %[kN/m2] vertical
stress increase exp 1.3kg
else
    q_inc_i = q_dike_oth*I_4_i;                                    %[kN/m2] vertical
stress increase other
end

G_d_i = Sig_s+q_inc_i;                                             %[kN/m2] increased
ground pressure (soil pressure + filled volume above)
FS_heave_impr = G_d_i/S_d;                                         %[-] factor of safety
with increased ground pressure
Con_eff_water_height = ((G_d_i-G_d)/y_w)*100;                      %[cm] control of
effective height compared to measured and determined effective water height -> W_cube)
                                                                   %     should be approx
zero if W_cube is equal to mass of V_cube (equal waterline -> 0.82~0.9kg)
%% Discretized global heave mechanism
%Discretization of heave zone
if discr_terzaghi == 1
D_d = 0.005;                                                         %[m] discretization
size
D_z = d_hscreen/D_d;                                                 %amount of vertical
zones
D_x = (0.5*d_hscreen)/D_d;                                           %amount of horizontal
zones
for z = 1:D_z+1
    for x = 1:D_x+1
        if z == 1                                                    %Nodes on pipe
            if x == 1
                depth(z,x) = 0;
                width(z,x) = 0;
            else
                depth(z,x) = 0;
                width(z,x) = (x-1)*D_d;
            end

            G_d_dis(z,x) = 0;                                        %Downward effective
soil pressure, zero because of pipe

            i_dis(z,x) = (phi_txt(x,z+1)-phi_txt(x,z))/D_d;          %Hydraulic gradient
from MSeep
            Sig_u_dis(z,x) = y_w*depth(z,x)+y_w*(phi_high-h_ground); %Pore water pressure
            Sig_sp_dis(z,x) = y_w*depth(z,x)*i_dis(z,x);             %Upward seepage
pressure
            S_d_dis(z,x) = Sig_u_dis(z,x)+Sig_sp_dis(z,x);           %Seepage pressure

            FS_heave_dis(z,x) = G_d_dis(z,x)/S_d_dis(z,x);

            if G_d_dis(z,x) <= S_d_dis(z,x)
                Extra_dis(z,x) = S_d_dis(z,x)-G_d_dis(z,x);          %Exceeded seepage
pressure
            else
                Extra_dis(z,x) = 0;
            end

        elseif z == 2                                                %Nodes below pipe
            depth(z,x) = (z-1)*D_d;
            width(z,x) = (x-1)*D_d;

            q_inc(z,x) = 0;
```

```
            Sig_s_dis(z,x) = y_w*depth(z,x);                          %Water pressure from
pipe
            Sig_T_dis(z,x) = Sig_s_dis(z,x);                          %Total vertical
pressure (only water from pipe)
            G_d_dis(z,x) = Sig_T_dis(z,x)+q_inc(z,x);                 %Downward pressure

            i_dis(z,x) = (phi_txt(x,z+1)-phi_txt(x,z))/D_d;           %hydraulic gradient
from MSeep
            Sig_u_dis(z,x) = y_w*depth(z,x)+y_w*(phi_high-h_ground); %Pore water pressure
            Sig_sp_dis(z,x) = y_w*depth(z,x)*i_dis(z,x);              %Upward seepage
pressure
            S_d_dis(z,x) = Sig_u_dis(z,x)+Sig_sp_dis(z,x);            %Seepage pressure
            FS_heave_dis(z,x) = G_d_dis(z,x)/S_d_dis(z,x);

            if G_d_dis(z,x) <= S_d_dis(z,x)
            Extra_dis(z,x) = S_d_dis(z,x)-G_d_dis(z,x);           %Exceeded seepage
pressure
            else
            Extra_dis(z,x) = 0;
            end
       else                                                        %All other nodes in
model
            depth(z,x) = (z-1)*D_d;
            width(z,x) = (x-1)*D_d;

            m_1 = L_dike/(B_dike);
            n_1 = depth(z,x)/((B_dike)/2);
            I_4_1 = (m_1*n_1)/sqrt(1+m_1^2+n_1^2);
            I_4_2 = (1+m_1^2+2*n_1^2)/((1+n_1^2)*(m_1^2+n_1^2));
            I_4_3 = asin(m_1/(sqrt(m_1^2+n_1^2)*sqrt(1+n_1^2)));
            I_4 = (2/pi)*(I_4_1*I_4_2+I_4_3);                         %vertical stress
increase component
            if W_cube == 1.3
                q_inc(z,x) = q_dike_w13*I_4;                          %vertical stress
increase rectangular loading formula
            else
                q_inc(z,x) = q_dike_oth*I_4;                          %vertical stress
increase rectangular loading formula
            end

            Sig_s_dis(z,x) = y_sat*depth(z,x);                        %Saturated soil
pressure
            G_d_dis(z,x) = Sig_s_dis(z)+q_inc(z,x);                   %Total vertical soil
pressure

            i_dis(z,x) = (phi_txt(x,z+1)-phi_txt(x,z))/D_d;           %hydraulic gradient
            Sig_u_dis(z,x) = y_w*depth(z,x)+y_w*(phi_high-h_ground); %Pore water pressure
            Sig_sp_dis(z,x) = y_w*depth(z,x)*i_dis(z,x);              %Upward seepage
pressure
            S_d_dis(z,x) = Sig_u_dis(z,x)+Sig_sp_dis(z,x);            %Seepage pressure

            FS_heave_dis(z,x) = G_d_dis(z,x)/S_d_dis(z,x);

            if G_d_dis(z,x) <= S_d_dis(z,x)
               Extra_dis(z,x) = S_d_dis(z,x)-G_d_dis(z,x);            %Exceeded seepage
pressure
            else
               Extra_dis(z,x) = 0;
            end
        end
```

```
    end
end
end

FS_heave_discr = mean(mean(FS_heave_dis));
%% Plotting figures
%Plotting values
disp(['The seepage pressure is ',num2str(S_d),' kN/m2']);
disp(['The dead load of the soil is ',num2str(G_d),' kN/m2']);
disp(['The dead load of the soil with the extra load is ',num2str(G_d_i),' kN/m2']);
disp(['The factor of safety for heave without extra stress is ',num2str(FS_heave)]);
disp(['The factor of safety for heave with extra load of dike structure is
',num2str(FS_heave_impr)]);
disp(['The average factor of safety of the discretized heave zone
',num2str(FS_heave_discr)]);

%Discretized plots
limits1 = [0,3];        %Colorbar limits figure 1
limits2 = [0,3];        %Colorbar limits figure 2

%Pressures
figure(1), clf(1)
subplot(1,3,1), hold on
title("Total vertical ground pressure")
surf(width, depth,
G_d_dis,"FaceAlpha",0.2,"FaceColor","interp","EdgeColor","interp","Marker",".","MarkerSize
",10)
set(gca,"YDir",'reverse')
colormap(jet)
c = colorbar;
c.Label.String = 'Pressure [kN/m2]';
set(gca,'clim',limits1([1,end]))
axis equal
axis([0 0.025 0 0.05])
ylabel("Depth [m]")
xlabel("Width [m]")
hold off

subplot(1,3,2), hold on
title("Total seepage pressure")
surf(width, depth,
S_d_dis,"FaceAlpha",0.2,"FaceColor","interp","EdgeColor","interp","Marker",".","MarkerSize
",10)
set(gca,"YDir",'reverse')
colormap(jet)
c = colorbar;
c.Label.String = 'Pressure [kN/m2]';
set(gca,'clim',limits1([1,end]))
axis equal
axis([0 0.025 0 0.05])
ylabel("Depth [m]")
xlabel("Width [m]")
hold off

subplot(1,3,3), hold on
title("Excess seepage pressure")
surf(width, depth,
Extra_dis,"FaceAlpha",0.2,"FaceColor","interp","EdgeColor","interp","Marker",".","MarkerSi
ze",10)
set(gca,"YDir",'reverse')
colormap(jet)
```

```
c = colorbar;
c.Label.String = 'Pressure [kN/m2]';
set(gca,'clim',limits1([1,end]))
axis equal
axis([0 0.025 0 0.05])
ylabel("Depth [m]")
xlabel("Width [m]")
hold off
sgtitle("Ground and seepage pressures on meso scale in heave failure zone")

%Factor of safety
figure(2), clf(2), hold on
title("Factor of safety in heave failure zone")
surf(width, depth,
FS_heave_dis,"FaceAlpha",0.2,"FaceColor","interp","EdgeColor","interp","Marker",".","Marke
rSize",10)
set(gca,"YDir",'reverse')
colormap(flipud(jet))
c = colorbar;
c.Label.String = 'Factor of safety [-]';
set(gca,'clim',limits2([1,end]))
axis equal
axis([0 0.025 0 0.05])
ylabel("Depth [m]")
xlabel("Width [m]")
hold off
```

A.2 MATLAB code for heave computation over varying water level

```
clear all, clc
%% Heave solution for full zone for multiple water heights and multiple pressures of dike
structure %%
%% Input variables
d_particle = 0.255;                                                    %[mm] (D50 - soil
particle size)
y_dry = 15.68;                                                         %[kN/m3] (unit weight
saturated soil)

W_cube = [0 0 1.3 1.6 1.9 2.2];                                      %[kg] (weight of cube or
only sheets)

phi_high = 0.20;                                                       %[m] (upside potential
heave screen MSeep (xcoor = ~0.215 ycoor = 0.15)
phi_low = [0.20 0.21651,0.23302,0.24954,0.26605,0.28256,0.29907];   %[m] (downside
potential heave screen MSeep (xcoor = ~0.215 ycoor = 0.10)
height = [0.20 0.25 0.30 0.35 0.40 0.45 0.50];                         %[m] (water height
measured from the bottom of the container
%% Parameters
% soil equation parameters
h_ground = 0.15;                %[m] (height soil layer)
d_hscreen = 0.05;               %[m] (depth heave screen)
g = 9.81;                       %[m2/s] (gravity constant)
y_w = 9.789;                    %[kN/m3] (unit weight water)
y_s = 25.99;                    %[kN/m3] (unit weight of soil particles) - 2650 kg/m3
k_z = 1.7e-04;                %[m/s] (permeability of the soil)
mu_visc = 0.0012;               %[kg/ms] (viscosity of water) (literatuur!)
n_por = 1-(y_dry/y_s);          %[-] (porosity percentage
y_sat = y_dry+n_por*y_w;        %[kN/m3] (unit weight of saturated soil)
rho_s = y_sat*101.971621;       %[kg/m3] (literatuur!)
rho_w = y_w*101.971621;         %[kg/m3] (literatuur!)
```

```
i_crit = (y_sat-y_w)/y_w;       %[-] (critical hydraulic gradient based on saturated soil)
%y_eff = (1-n_por)*(y_s-y_w);   %[-] (effective unit weight soil based on porosity)
%i_crit = y_eff/y_w; %critical  %[-] (critical hydraulic gradient on porosity)

% vertical stress parameters
L_dike = 0.492;                 %[m] (length bottom sheet dike)
B_dike = 0.15;                  %[m] (width bottom sheet dike)
d_dike = 0.005;                 %[m] (thickness sheet)
L_cube = 0.15;                  %[m] (length dike cube)
Lb_cube = 0.144;                %[m] (innerlength dike cube)
Hb_cube = 0.147;                %[m] (innerheight dike cube)
rho_plexi = 1190;               %[kg/m3] (density plexi)

L_tsheet = 0.45;                %[m] (length thin sheet)
B_tsheet = 0.12;                %[m] (width thin sheet)
d_tsheet = 0.004;               %[m] (thickness thin sheet)

%% Determination of volumes,of dike structure
h_imm_cube = phi_high-(h_ground+d_dike+2*d_tsheet);           %[m] (immersed depth of
cube)

Tot_V_dike = L_dike*B_dike*(phi_high-h_ground);               %[m3] (filled volume above
loaded cover plate)
V_bsheet = L_dike*B_dike*d_dike;                             %[m3] (volume of plexi base
sheet)
V_esheet = 2*L_tsheet*B_tsheet*d_tsheet;                     %[m3] (volume of plexi extra
sheet)
V_cube = L_cube^2*h_imm_cube;                                %[m3] (immersed volume of
cube
V_water_pla = Tot_V_dike-V_bsheet;                           %[m3] (water volume in
plates exp)
V_water_w13 = Tot_V_dike-(V_bsheet+3*V_cube);                %[m3] (water volume in
w_cube 1.3 kg exp -> "gele doekjes")
V_water_oth = Tot_V_dike-(V_bsheet+V_esheet+3*V_cube);       %[m3] (water volume in other
exp)
%% Vertical load component
m_1_i = L_dike/(B_dike);
n_1_i = (d_hscreen)/((B_dike)/2);
I_4_1_i = (m_1_i*n_1_i)/sqrt(1+m_1_i^2+n_1_i^2);
I_4_2_i = (1+m_1_i^2+2*n_1_i^2)/((1+n_1_i^2)*(m_1_i^2+n_1_i^2));
I_4_3_i = asin(m_1_i/(sqrt(m_1_i^2+n_1_i^2)*sqrt(1+n_1_i^2)));
I_4_i = (2/pi)*(I_4_1_i*I_4_2_i+I_4_3_i);                     %vertical stress increase
component
%% Original global heave mechanism
%Global stability condition
for kg = 1:length(W_cube)                                                %Loop for all
extra pressure by dike structure
    %Added pressures values for dike structure
    if kg == 1
        q_dike(kg) = 0;                                                  %[kN/m2] Stress
of dike structure, regular heave
        Sig_w = y_w*(phi_high-h_ground);
        q_inc_i(kg) = Sig_w;

        Sig_s = y_sat*d_hscreen;                                         %[kN/m2]
Saturated soil pressure
        G_d(kg) = Sig_w+Sig_s;                                           %[kN/m2] Total
vertical soil pressure
    elseif kg == 2
        Tot_M_pla = V_water_pla*rho_w + V_bsheet*rho_plexi;
```

```
        q_dike(kg) = ((Tot_M_pla*g)/1000)/(L_dike*B_dike);                  %[kN/m2] Stress
of dike structure, only sheets and water
        q_inc_i(kg) = q_dike(kg);                                           %[kN/m2]
vertical stress increase rectangular loading formula

        Sig_s = y_sat*d_hscreen;                                            %[kN/m2]
Saturated soil pressure
        G_d(kg) = Sig_s+q_inc_i(kg);                                        %[kN/m2] Total
vertical soil pressure
    elseif kg == 3 && W_cube(kg) == 1.3
        Tot_M_w13 = V_water_w13*rho_w + V_bsheet*rho_plexi + 3*W_cube(kg);
        q_dike(kg) = ((Tot_M_w13*g)/1000)/(L_dike*B_dike);                 %[kN/m2] Stress
of dike structure, 1.3kg exp
        q_inc_i(kg) = q_dike(kg)*I_4_i;                                     %[kN/m2]
vertical stress increase rectangular loading formula

        Sig_s = y_sat*d_hscreen;                                            %[kN/m2]
Saturated soil pressure
        G_d(kg) = Sig_s+q_inc_i(kg);                                        %[kN/m2] Total
vertical soil pressure
    else
        Tot_M_oth = V_water_oth*rho_w + (V_bsheet+V_esheet)*rho_plexi + 3*W_cube(kg);
%[kN/m2] Stress of dike structure, other exp
        q_dike(kg) = ((Tot_M_oth*g)/1000)/(L_dike*B_dike);
        q_inc_i(kg) = q_dike(kg)*I_4_i;                                     %[kN/m2]
vertical stress increase rectangular loading formula

        Sig_s = y_sat*d_hscreen;                                            %[kN/m2]
Saturated soil pressure
        G_d(kg) = Sig_s+q_inc_i(kg);                                        %[kN/m2] Total
vertical soil pressure
    end
end

for p = 1:length(phi_low)
    %Seepage pressure in heave zone
    i_ver(p) = (phi_low(p)-phi_high)/d_hscreen;                             %[-]
vertical hydraulic gradient for different water height from MSeep
    U_sig = y_w*(d_hscreen+(phi_high-h_ground));                            %[kN/m2]
Pore water pressure
    Sp_sig(p) = y_w*i_ver(p)*d_hscreen;                                     %[kN/m2]
Upward seepage pressure
    S_d(p) = Sp_sig(p)+U_sig;                                               %[kN/m2]
Seepage pressure
end

for p = 1:length(phi_low)
    for kg = 1:length(W_cube)
        FS_heave(p,kg) = G_d(kg)/S_d(p);                                    %[-] Factor
of safety for different water heights and different stresses of dike structures (one
column has all values for one water height, one row has all values for one stress value of
dike structure)
    end
end
%% Line equations
%calculating linear line equations for (critical) seepage pressures and total vertical
soil pressures
a_seep = (S_d(7)-S_d(1))/(height(7)-height(1));
b_seep = S_d(1)-height(1)*a_seep;
f_seep = @(x) a_seep*x+b_seep;
f_ground0 = @(x) x*0+G_d(1);
```

```
f_ground_struc = @(x) x*0+G_d(2);
f_ground1 = @(x) x*0+G_d(3);
f_ground2 = @(x) x*0+G_d(4);
f_ground3 = @(x) x*0+G_d(5);
f_ground4 = @(x) x*0+G_d(6);

a_ver = (i_ver(7)-i_ver(1))/(height(7)-height(1));
b_ver = i_ver(1)-height(1)*a_ver;
f_ver = @(x) a_ver*x+b_ver;
f_crit = @(x) x*0+i_crit;

f_fos1 = @(x) x*0+1;
f_fos15 = @(x) x*0+1.5;
f_fos2 = @(x) x*0+2;

%% Intersecting points
% critical heave point for hydraulic gradient and total vertical soil pressures
wh_i_crit = ((i_crit-b_ver)/a_ver)*1000
wh_0 = ((G_d(1)-b_seep)/a_seep)*1000
wh_struc = ((G_d(2)-b_seep)/a_seep)*1000
wh_g013 = ((G_d(3)-b_seep)/a_seep)*1000
wh_g016 = ((G_d(4)-b_seep)/a_seep)*1000
wh_g019 = ((G_d(5)-b_seep)/a_seep)*1000
wh_g022 = ((G_d(6)-b_seep)/a_seep)*1000

%% Plotting figures
figure(10),clf(10)
subplot(2,1,1),hold on
title("Ground pressure and seepage pressure")
xlabel("Upstream water height [m]")
ylabel("Pressure [kN/m2]")
fplot(f_seep)
fplot(f_ground0)
fplot(f_ground_struc)
fplot(f_ground1)
fplot(f_ground2)
fplot(f_ground3)
fplot(f_ground4)
legend("Seepage pressure","Ground pressure","Extra structural load (cover plates)","Extra
cube weight (1.3 kg)","Extra cube weight (1.6 kg)","Extra cube weight (1.9 kg)","Extra
cube weight (2.2 kg)","Location","northeastoutside")
axis([0.2 0.5 0 4])
hold off

subplot(2,1,2), hold on
title("Vertical hydraulic gradient")
xlabel("Upstream water height [m]")
ylabel("Hydraulic gradient [-]")
fplot(f_ver)
fplot(f_crit)
legend("Hydraulic gradient","Critical hydraulic gradient","Location","northeastoutside")
axis([0.2 0.5 0 4])
hold off

figure(11),clf(11),hold on
title("Factor of safety")
xlabel("Upstream water height [m]")
ylabel("Factor of safety [-]")
plot(height,FS_heave(:,1))
plot(height,FS_heave(:,2))
plot(height,FS_heave(:,3))
```

```
plot(height,FS_heave(:,4))
plot(height,FS_heave(:,5))
plot(height,FS_heave(:,6))
fplot(f_fos1,"Color","k")
fplot(f_fos15,"Color","k")
fplot(f_fos2,"Color","k")
legend("Standard heave","Extra structural load (cover plates)","Individual cube weight
(1.3 kg)","Individual cube weight (1.6 kg)","Individual cube weight (1.9 kg)","Individual
cube weight (2.2 kg)","Location","northeastoutside")
axis([0.2 0.5 0 3])
hold off

%% plot breakpoint figure
exp_fail = [37.2 39.1 44.5 46.4 45.4 46.1];
exp_dis = [33.3 38.7 44 46.2 44.5 45.8];
ana = [wh_0 wh_struc wh_g013 wh_g016 wh_g019 wh_g022]/10;
exp_num = ["Classical heave" "Heave with cover plates" "Heave - 1.3 kg" "Heave - 1.6 kg"
"Heave - 1.9 kg" "Heave - 2.2 kg"];

fail_reg = polyfit([q_inc_i(2:6)],[exp_fail(2:6)],1);
dis_reg = polyfit([q_inc_i(2:6)],[exp_dis(2:6)],1);
ana_reg = polyfit([q_inc_i(2:6)],[ana(2:6)],1);

fail_y = polyval(fail_reg,[q_inc_i(2:6)]);
dis_y = polyval(dis_reg,[q_inc_i(2:6)]);
ana_y = polyval(ana_reg,[q_inc_i(2:6)]);

figure(12),clf(12),hold on
title("Critical upstream water height")
xlabel("Vertical load on the soil [kN/m2]")
ylabel("Upstream water height [cm]")
plot([q_inc_i(1:6)],[exp_fail(1:6)],"r-o","MarkerSize",5,"MarkerFaceColor","r")
plot([q_inc_i(1:6)],[exp_dis(1:6)],"b-o","MarkerSize",5,"MarkerFaceColor","b")
plot([q_inc_i(1:6)],[ana(1:6)],"g-o","MarkerSize",5,"MarkerFaceColor","g")
plot([q_inc_i(2:6)],fail_y,"r--")
plot([q_inc_i(2:6)],dis_y,"b--")
%plot([verl_ex(3:6)],ana_y,"g--")
axis([q_inc_i(1) q_inc_i(6) 25 50])
legend("Experimental - failure","Experimental - deformation","Analytical","Regression line
- failure","Regression line - deformation","Location","northeastoutside")
hold off

%% plot head figure
water_height = [23 28 35.8 28.4 33 38 26 31 37.4];
piezo1_5 = [11.8 16.1 22.1 15.2 20 23 14.5 18.1 23.4];
piezo2 = [15.8 20 25 18 22.7 24.5 19.3 22.9 26.9];
piezo3 = [16 20 25 18.5 22.9 24.5 17.8 21.3 22.8];
piezo4 = [16 20 25.2 17.2 22 24.1 19.1 22.8 26.1];
Mseep_10 = [16.668 19.448 23.786 19.671 22.229 25.009 18.336 21.117 24.675];
Mseep_5 = [11.985 15.294 20.455 15.558 18.602 21.91 13.97 17.279 21.513];

figure(13),clf(13),hold on
title("Hydraulic head measurements")
xlabel("Upstream water height [cm]")
ylabel("Measured pressure [cm]")
plot(water_height,piezo1_5,"r.","MarkerSize",12)
plot(water_height,piezo2,"b.","MarkerSize",12)
plot(water_height,piezo3,"b*","MarkerSize",6)
plot(water_height,piezo4,"bo","MarkerSize",4)
plot(water_height,Mseep_5,'r')
plot(water_height,Mseep_10,'b')
```

```
legend("Piezo 1 (depth 5cm)","Piezo 2 (depth 10cm)","Piezo 3 (depth 10cm)","Piezo 4 (depth
10cm)","MSeep (depth 5cm)","MSeep (depth 10cm)","Location","northeastoutside")
axis([22 39 10 28])
hold off
```

Appendix B

Laboratory results of soil characteristic tests

B.1 Laboratory results of soil proctor test

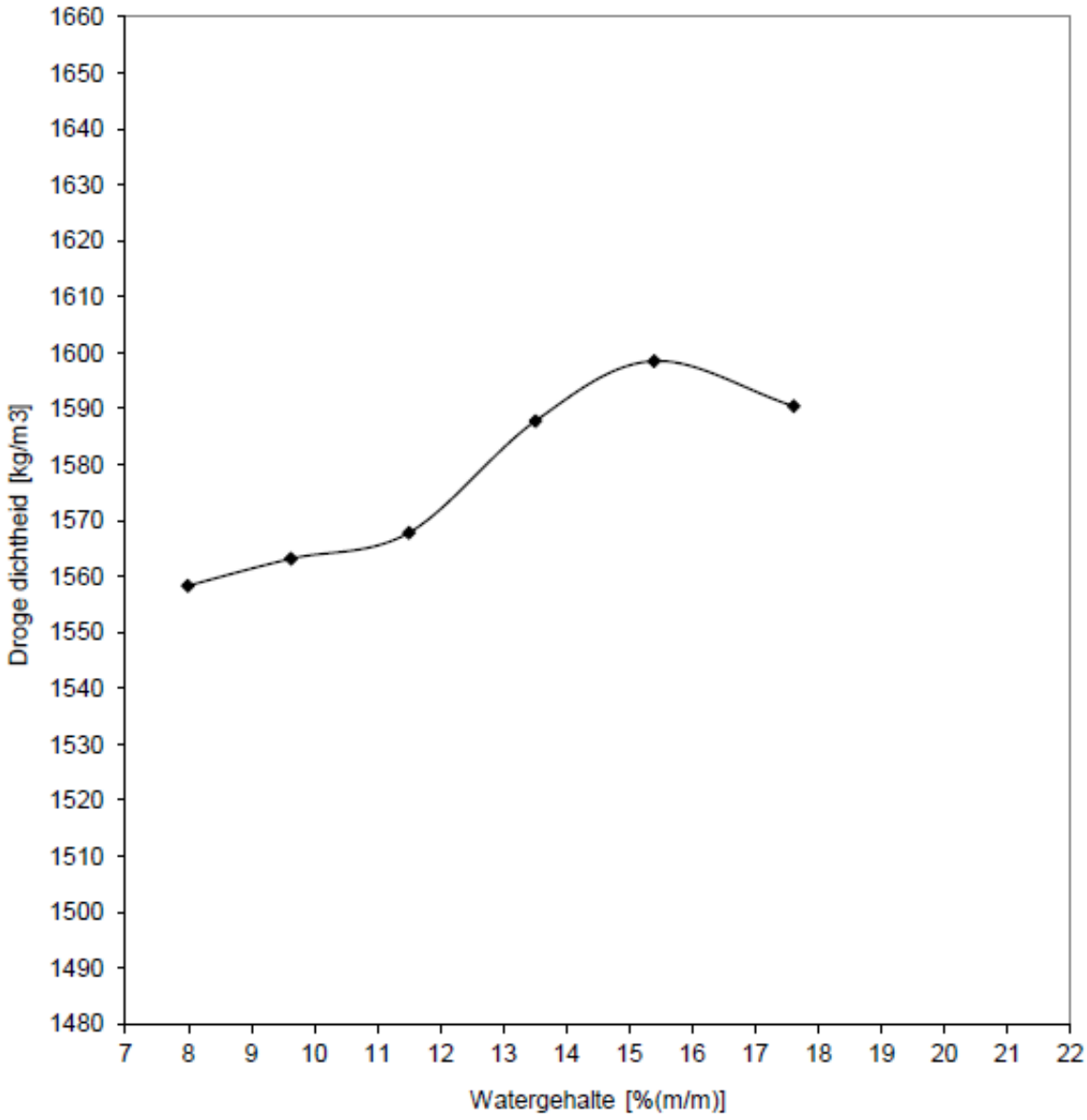

			Punt1	8.0	1558
			Punt2	9.6	1563
			Punt3	11.5	1568
Monster:	Lukas		Punt4	13.5	1588
Maximum droge dichtheid:	1599	kg/m^3	Punt5	15.4	1599
Optimum watergehalte:	15.4	% (m/m)	Punt6	17.6	1590

Methode conform proef 9 STD. RAW (Q)

De met 'Q' gemerkte verrichtingen zijn geaccrediteerd door RvA.

NORMALE PROCTORPROEF
Project John en stagiare

Opdr. nr. 6422-220279
Gecontroleerd door: JKK

B.2 Laboratory results of soil permeability test

ONDERZOEKSRAPPORT			
Project	Dijkzonealliantie NL Nederbetuwe (consulting)		
Opdrachtgever	Fugro NL LAND B.V.	Opdrachtnummer	6422-220279
Contactpersoon	Lukas Raadschelders	Datum rapport	21-06-2023
Monstername	Uitgevoerd door Opdrachtgever	Datum ontvangst	13-06-2023

ONDERZOEK MONSTERS			
Monster	Omschrijving	Diepte in m-mv.	Opmerkingen
1	Lukas-MM1		
2			
3			
4			
5			

RESULTATEN							
Parameter	Monsternummer					Eenheid	Methode van onderzoek
	1	2	3	4	5		
Waterdoorlatendheid	1.7E-04					m/s	Constant Head
Waterdoorlatendheid						m/s	Falling Head

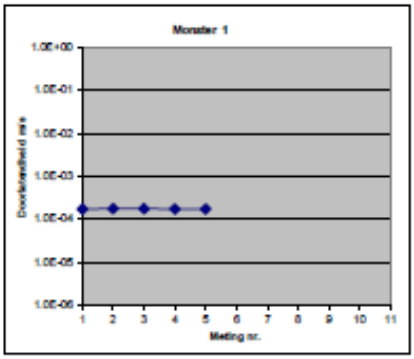

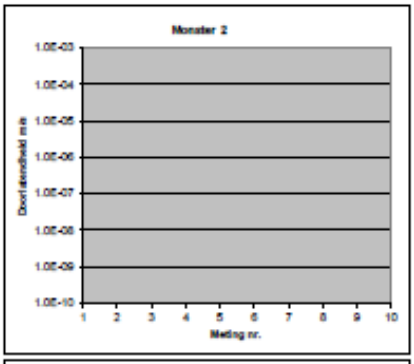

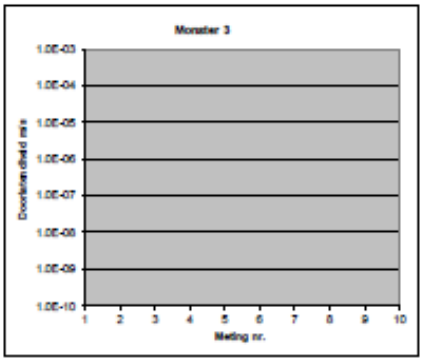

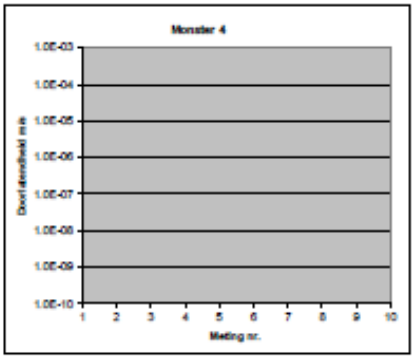

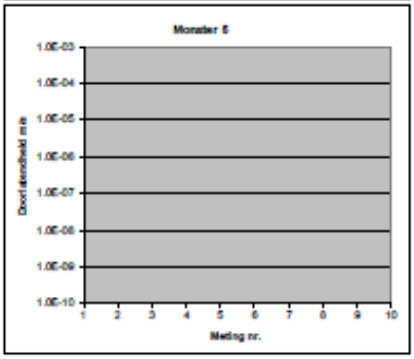

OPMERKINGEN
De met "Q" gemerkte verrichtingen zijn erkend door RvA

Opgesteld door:	JKK	Gecontroleerd:	AWG	Opdr. nr.	6422-220279

B.3 Laboratory results of soil sieving test

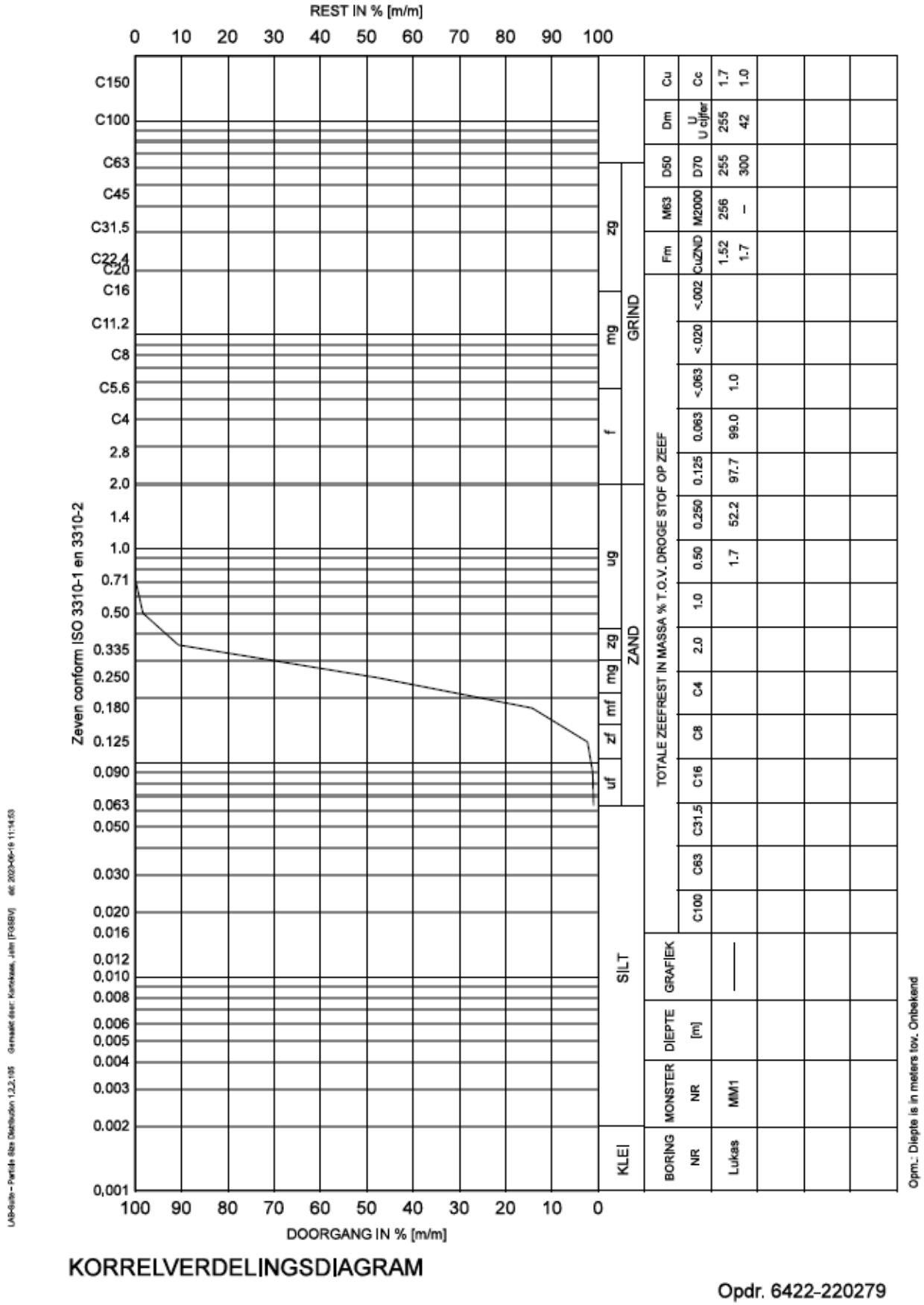

Project Nr	: 6422-220279	Datum	: 19-06-23 09:04:08
Boring	: Lukas	Laborant	: Kortekaas, John [FGSBV]
Monster	: MM1		
Diepte			
Totale massa	: 159.21 gram		
Opmerkingen			

Diameter	: 2,000	1,400	1,000	0,710	0,500	0,355	0,250	0,180	0,125	0,090	0,063
Gram	: 0,00	0,03	0,02	0,18	2,71	14,88	83,16	138,46	155,49	157,33	157,59
Procenten	: 100,0	100,0	100,0	99,9	98,3	90,7	47,8	14,3	2,3	1,2	1,0

M2000	:	0,0 mm	D50	:	255 µm.	Fijnheidsgetal	:	1,52
M63	:	256 µm.	Cu	:	1,7	U cijfer	:	42
Dm	:	255 µm.	Cc	:	1.0			
Zandfractie			Cu	:	1.7			
			Cc	:	1.0			